Heat transfer coefficients of laminar, transitional, quasi-turbulent and turbulent flow in circular tubes

J.P. Meyer*, M. Everts, N. Coetzee, K. Grote, and M. Steyn

Department of Mechanical and Aeronautical Engineering, University of Pretoria, Private Bag X20, Hatfield 0028, Pretoria, South Africa.

**Corresponding author:* Email: josua.meyer@up.ac.za, Phone: +27 12 420 3104

Highlights

- Turbulent and quasi-turbulent heat transfer and pressure drop experimental data
- Quantified uncertainties of variables
- Nusselt number correlation for quasi-turbulent and turbulent flow
- Single Nusselt number correlation for laminar to turbulent flow in horizontal tubes

Abstract

Several well-known correlations to determine the heat transfer coefficients of quasi-turbulent and turbulent flow in smooth tubes are available in literature. However, when these correlations are compared with each other, the results vary over a considerable range. The purpose of this study was therefore to conduct heat transfer and pressure drop experiments in the quasi-turbulent and turbulent flow regimes and to develop an accurate heat transfer correlation that can be combined with recently developed laminar and transitional flow correlations to obtain a single correlation that is valid for all flow regimes. A total of 1 180 experimental data points were collected from careful experiments that were conducted ourselves using two different test section configurations. The first test section configuration consisted of a tube-in-tube test section on which the wall temperatures were obtained either indirectly using the Wilson plot method or by direct surface temperature measurements. The second test section configuration consisted of single tubes being electrically heated at a constant heat flux. Different test sections covering a range of tube diameters from 4 mm to 19 mm and a range of tube lengths from 1 m to 9.5 m, were used. Experiments were conducted from a Reynolds number of 2 445, which corresponded to the start of the quasi-turbulent flow regime, up to 220 800, which was well into the turbulent flow regime. Water, as well as different concentrations of multi-walled carbon nanotubes, were used as the test fluid, which gave a Prandtl number range of 3-10. A new correlation was developed that could estimate 95% of all the experimental data points within 10% and an average deviation of less than 5%. Furthermore, it was able to predict experimental data in literature with a Prandtl number range of 0.47-276 and Reynolds number range of 3 000-401 600 with an average deviation of 14%.

Keywords: Nusselt number, friction factor, Reynolds number, heat transfer, pressure drop, circular, turbulent, quasi-turbulent, transition, laminar, smooth tubes, uncertainty

Nomenclature

A	Area
C_p	Specific heat capacity
C	Wilson Plot coefficient/ constant used in correlations
c	Coefficient used in correlations
D	Diameter of tube
f	Friction factor
g	Gravitational acceleration
Gr	Grashof number
Gz	Graetz number
h	Heat transfer coefficient
j	Colburn j-factor
K	Temperature correction factor ($K = (Pr/Pr_w)^{0.11}$)
k	Thermal conductivity
L	Length of tube
Lt	Thermal entrance length
M	Measurement
$\dot{m}$	Mass flow rate
Nu	Nusselt number
ΔP	Pressure drop
Pr	Prandtl number
$\dot{q}$	Heat flux/ constant heat flux boundary condition
R^2	Coefficient of determination
Re	Reynolds number
T	Temperature
Ts	Constant surface temperature boundary condition
V	Fluid velocity

Greek Symbols

β	Thermal expansion coefficient
γ	Intermittency factor
ε	Surface roughness height
δ	Uncertainty
μ	Dynamic viscosity of fluid
ν	Kinematic viscosity
ρ	Density of fluid

Superscripts

m, n, p	Exponents used in correlations
p	Wilson Plot variable

Subscripts

b	bulk
c	Cross-section
cor	Correlation
exp	Experimental
i	Inlet/ inner/ inside
lam	Laminar
MCD	Mixed convection thermal entrance length
o	Outlet/ outer/ annulus
ref	Reference
turb	Turbulent
w	Wall

Abbreviations

BC	Boundary condition
TM	Temperature measurements method
WP	Wilson Plot method

1. Introduction

Turbulent heat transfer in circular tubes has been well researched and documented over the past 100 years. Fig. 1 compares the number of publications containing the phrase “turbulent heat transfer” in the title, abstract or keywords per year according to Scopus. This figure indicates that although the topic of turbulent heat transfer in tubes has been well researched and documented, it is still gaining interest.

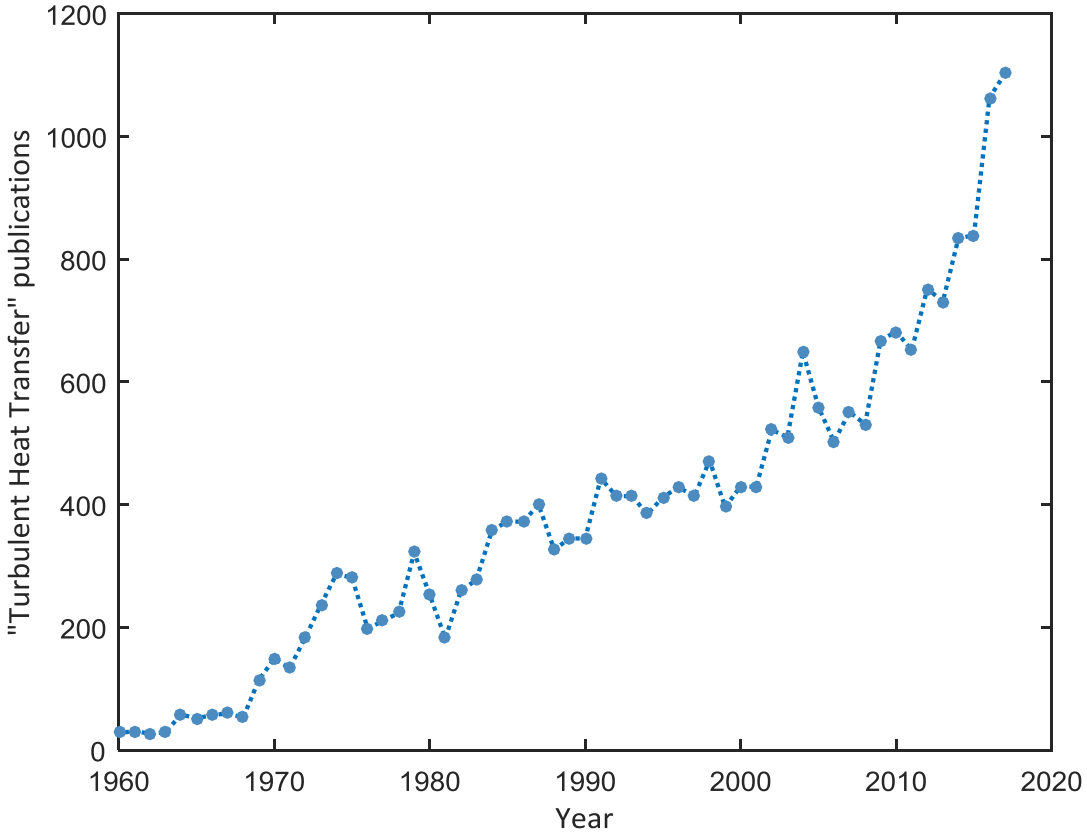

Fig. 1: Number of publications containing the phrase "turbulent heat transfer" in the title, abstract or keywords per year according to Scopus (Accessed: May 2018).

Although many turbulent heat transfer data have been recorded and many correlations have been developed in the past 100 years, there is still a considerable large discrepancy in the agreement of these studies and correlations with each other. Table 1 gives a summary of the well-known and widely used turbulent heat transfer correlations. The experimental data that are readily available in literature and that was used to develop the correlations in Table 1 are summarised in Table 2.

In 1915, Nusselt suggested the following form for Nusselt number correlations [1]:

$$Nu = cRe^{m}Pr^{n}\left(\frac{D}{L}\right)^{p} \tag{1}$$

With the aim of producing a single equation to accurately predict the heat transfer coefficients in both heating and cooling applications, Dittus and Boelter [2] performed experiments of their own and combined their data with the data of previous studies [3-6]. Because the D/L-values in the source data were very small, the D/L term in Eq. (1), which was associated with entry effects, was neglected. The resulting correlation (Eq. (2) in Table 1) contained an exponent, n, to predict the heating and cooling data separately, which enabled good agreement with the previous data sets.

Table 1: Summary of well-known and widely used turbulent heat transfer correlations

Dittus and Boelter [2] $Nu = 0.023Re^{0.8}Pr^{n}$ n = 0.3 for cooling n = 0.4 for heating $3\times10^3 < Re < 10^6$, $0.7 < Pr < 120$ Source data: [3-6], [7, 8]*	(2)
Colburn [9] $Nu = 0.023Re^{0.8}Pr^{1/3}$ $Re > 10^4$, $0.7 < Pr < 160$ Source data: [3-5, 10-17], [18]*	(3)
Sieder and Tate [19] $Nu = 0.027Re^{0.8}Pr^{1/3}\left(\frac{\mu}{\mu_w}\right)^{0.14}$ $Re > 10^4$, $0.7 < Pr < 17\,600$ Source data: [3, 16, 17, 20-24], [18, 25]	(4)
Hausen [1] $Nu = 0.037(Re^{0.75} - 180)Pr^{0.42}\left[1 + \left(\frac{D}{L}\right)^{2/3}\right]\left(\frac{\mu}{\mu_w}\right)^{0.14}$ $2\,300 < Re < 10^6$, $0.6 < Pr < 10^3$ Source data: [3, 16, 17, 20-24], [18, 25]*	(5)
Petukhov [26] $Nu = \frac{\left(\frac{f}{8}\right)RePr}{1.07 + 12.7\sqrt{\frac{f}{8}}(Pr^{2/3} - 1)}$ $10^4 < Re < 5\times10^6$, $0.5 < Pr < 2\,000$ Source data: [27-30]	(6)
Gnielinski [31] $Nu = \frac{\left(\frac{f}{8}\right)(Re - 1000)Pr}{1 + 12.7\sqrt{\frac{f}{8}}(Pr^{2/3} - 1)}\left[1 + \left(\frac{D}{L}\right)^{2/3}\right]K$ $K = \left(\frac{Pr}{Pr_w}\right)^{0.11}$ $2\,300 < Re < 10^6$, $0.6 < Pr < 10^5$ Source data: [3, 14, 16, 17, 20, 23, 29, 32-34], [18, 25, 35-38]*	(7)

*It was not possible for the authors to confirm these references because of unavailability.

Table 2: Summary of the readily available turbulent experimental data used to develop the well-known turbulent Nusselt number correlations in Table 1. *Ts* refers to a constant surface temperature boundary condition and $\dot{q}$ to a constant heat flux boundary condition.

	Test fluid	Boundary condition	Heating/ cooling	Reynolds number	Prandtl number	Employed by
Webster [39]	Water	*Ts*	Heating	4 256 – 51 059	3.7 – 8.8	McAdams and Frost [6] Dittus and Boelter [2]
Morris and Whitman [3]	Water	*Ts*	Heating	10 107 – 38 816	2.9 – 3.1	Dittus and Boelter [2] Colburn [9] Sieder and Tate [19] Gnielinski [31]
	Gas oil	*Ts*	Heating	2 282 – 30 011	32.8 – 47.2	
	Straw oil	*Ts*	Heating	754 – 13 145	57.7 – 224	
	Light motor oil	*Ts*	Heating	620 – 4 303	203 – 782	
	Gas oil	*Ts*	Cooling	3 634 – 44 149	18.2 – 31.2	
	Straw oil	*Ts*	Cooling	1 327 – 45 265	8.6 – 99.2	
	Light motor oil	*Ts*	Cooling	947 – 9 363	61.5 – 229	
Clapp and FitzSimons [20]	Water	*Ts*	Heating	13 307 – 60 147	1.7 – 6.4	Sieder and Tate [19] Gnielinski [31]
	Velocite B	*Ts*	Heating	521 – 7 093	72.1 – 397	
	Water	*Ts*	Cooling	19 098 – 59 650	14.9 – 5.0	
	Velocite B	*Ts*	Cooling	840 – 7 218	71.1 – 105	
Lawrence and Sherwood [23]	Water	*Ts*	Heating	4 113 – 140 005	2.2 – 8.9	Sieder and Tate [19] Gnielinski [31]
Sherwood *et al*. [17]	Light hydrocarbon oil	*Ts*	Heating	280 – 5 570	102 – 221	Colburn [9] Sieder and Tate [19] Gnielinski [31]
Sherwood and Petrie [16]	Water	*Ts*	Heating	2 800 – 113 000	3.9 – 367	Colburn [9] Sieder and Tate [19] Gnielinski [31]
	Acetone	*Ts*	Heating	944 – 89 500	3.7 – 4.4	
	Benzene	*Ts*	Heating	206 – 86 700	6.3 – 8.2	
	Kerosene	*Ts*	Heating	256 – 31 800	20.6 – 23.9	
	n-Butyl alcohol	*Ts*	Heating	297 – 32 500	35.5 – 897	
Stone *et al*. [32]	*n*-Hexadecane	$\dot{q}$	Heating	12 500 – 223 800	11.6 – 18.6	Gnielinski [31]
	Di(2-ethylhexyl) adipate	$\dot{q}$	Heating	13500 – 124 200	15.1 – 24.2	
	Biphenyl	$\dot{q}$	Heating	31 500– 401 600	4.1 – 6.4	
	Monoisopropylbiphenyl	$\dot{q}$	Heating	18 500 – 349 800	5.1 – 15.5	

Colburn [9] broke new ground by making use of dimensionless variables such as Reynolds, Prandtl and Nusselt number to reduce the number of variables in the calculation of the heat transfer coefficients. In addition to this, Colburn recognised the relationship between heat transfer and pressure drop, as well as the effect that the wall temperature has on fluid properties. The proposed correlation (Eq. (3)) was therefore based on the Chilton-Colburn analogy [40] and the fluid properties were calculated at the film temperature instead of the bulk temperature. It should be noted that although Eq. (2) was obtained by correlating experimental data and Eq. (3) was obtained through a theoretical approached combined with experimental pressure drop data, the two correlations are similar. The difference is that the Prandtl numbers in the correlation of Dittus and Boelter [2] are calculated at the bulk fluid temperature, while Colburn [9] based the Prandtl numbers on the film temperature. Another important observation made by Colburn [9] was that the heat transfer coefficients decreased and deviated from the straight line (on a log-log plot) for Reynolds numbers between 2 300 and 10^4. A "resume chart", which could be used to obtain the heat transfer coefficients in this region, was proposed because a suitable correlation for this region could not be developed.

Sieder and Tate [19] incorporated the viscosity ratio (μ/μ_w), which accounted for the viscosity gradient of the fluid inside the tube. A coefficient of 0.14 was found to be suitable for both heating and cooling conditions. However, other investigations yielded different values for the coefficient [41]. For example, Petukhov [26] suggested coefficients of 0.11 and 0.25 for heating and cooling, respectively, while Büyükalaca and Jackson [42] proposed that the coefficient should be a function of Reynolds number. Similar to Dittus and Boelter [2], Sieder and Tate [19] calculated the fluid properties (except for the viscosity at the tube wall) at the bulk fluid temperature. The decrease in heat transfer coefficients at lower Reynolds numbers that was observed by Colburn [9], was also observed by Sieder and Tate [19] between Reynolds numbers of 2 000 and 10^4 and the authors explained that these data formed part of the transitional flow regime. However, according to a recent study conducted by Everts and Meyer [43] these data fell into the quasi-turbulent flow regime, between the transitional and turbulent flow regimes.

To account for the heat transfer coefficients in the transitional flow regime, Hausen [1] proposed the following form for Nusselt number correlations:

$$Nu \propto (Re^m - C) \tag{8}$$

where m and C are constants which can be obtained experimentally. This form made it possible to obtain a single correlation for transitional and turbulent flow (Eq. (5)). However, it was found that Eq. (5) underpredicted the experimental data at lower Reynolds numbers in the transitional flow regime, as well as when short tubes were considered [31].

In an effort to predict the turbulent heat transfer behaviour more accurately, the next phase of heat transfer research resulted in more work being undertaken in the field where analytical methods were used to solve for the equations. Petukhov [26] performed a considerable amount of analyses, using existing

data sets as well as producing some data of his own, to obtain a correlation (Eq. (6)) which accounted for the effect that the friction factor has on heat transfer in the system. Although Eq. (6) was more complex than the previous correlations (Eqs. (2)-(5)), it provided an alternative to the Nusselt number correlation form proposed by Nusselt (Eq. (1)).

Gnielinski [31] evaluated the existing correlations and experimental data available for turbulent flow. A new correlation (Eq. (7)) with a form similar to Petukhov [26] was proposed. However, the Reynolds number compensation (Eq. (8)) suggested by Hausen [1], a temperature correction factor ($K = (Pr/Pr_w)^{0.11}$) similar to what was suggested by Sieder and Tate [19], and a term $[1 + (D/L)^{2/3}]$ were incorporated. Similar to Hausen [1], it was found that in relatively short tubes, the heat transfer coefficients were dependent on the tube length due to the development of the hydraulic and thermal boundary layers, therefore the term $[1 + (D/L)^{2/3}]$ was included. Eq. (7) was deemed to be considerably accurate because it was able to predict nearly 90% of the approximately 800 experimental data points in literature within 20%. However, it should be noted that the uncertainties of these experimental data points in literature were not available. Furthermore, at a Nusselt number of approximately 700, the experimental data used by Gnielinski [31] deviated up to 50%. To account for the transitional flow regime, Gnielinski [44] proposed to use linear interpolation for Reynolds numbers between 2 300 and 4 000, and Eq. (7) for Reynolds numbers greater than 4 000.

Several other turbulent heat transfer correlations were also developed in the past decade. These correlations not only accounted for variable fluid properties [41, 45], but also for heat transfer coefficients that fell in the quasi-turbulent flow regime [46-49]. However, the majority of these correlations were obtained numerically [46-48, 50] or are restricted to certain fluids [45, 49, 51-54].

Table 2 indicates that the experimental data that were used to develop the correlations in Table 1 were obtained using various test fluids, but the experiments were only conducted up to a Reynolds number of 401 600 [32]. Furthermore, in many cases the experiments conducted with the highest Prandtl number fluids were not necessarily in the turbulent flow regime, but in the laminar flow regime (owing to the significant increase in pressure drop with increasing Reynolds number when high viscosity fluids were used). To the authors' best knowledge Morris and Whitman [3] conducted turbulent experiments with the maximum Prandtl number of 276 using light motor oil. Therefore, although Table 1 indicates that some correlations are valid op to Reynolds numbers of 5×10^6 and Prandtl numbers of 10^5, these ranges were obtained by extrapolation and not using experimental data points.

In general it is assumed that the correlations of Gnielinski [31] and Petukhov [26] are the most accurate as they were most recently developed and are well-known, while the older correlations should be less accurate and thus be phased out. However, a search (May 2018) on Scopus showed that the older correlations are still actively being used by many researchers when validating smooth tube experimental data. Dittus and Boelter [55] had 292 citations, Colburn [56] 49 citations, Sieder and Tate [19] 1 119 citations, Petukhov [26] 865 citations and Gnielinski [31] had 155 citations. Therefore, based on the number of citations, the correlation of Sieder and Tate [19] seemed to be the most utilised correlation.

However, a large amount of the initial work of Gnielinski and Petukhov was published in the German and Soviet literature and in textbooks, therefore the number of citations to their work were probably underestimated according to cited literature. For example, the work of Gnielinski was published in 1976 in the journal of International Chemical Engineering with permission from the VDI-Verlag GmbH; however, this paper is not on the Scopus database. Thus, there is no clear evidence from literature (based on number of citations) which one of the many correlations are in general the most utilised and most accurate.

When comparing the different correlations, it was found that for a Prandtl number of 7, the Nusselt numbers obtained using the correlations of Petukhov [26] and Gnielinski [31] were within 5% at a fixed Reynolds number. However, at a Reynolds Number of 10 000, the deviation between the Nusselt numbers obtained using the correlations of Sieder and Tate [19] and Petukhov [26] was more than 50%. This deviation gradually decreased to 40% at a Reynolds number of 200 000.

It should also be noted that in the period of 1922 to 1936, when the majority of the experiments that formed the basis of the work of many scholars in terms of improvements and refinements were conducted, the execution of uncertainty analyses was not a requirement in scholarly journals. Therefore, the uncertainties of convective heat transfer correlations in smooth tubes, which are widely published in heat transfer textbooks and used for validation and comparison studies today, are in general not readily available. Furthermore, the measuring instrumentation available today are more accurate than a century ago, therefore it should be possible to not only conduct more accurate experiments, but also to derive a more accurate correlation with a quantified uncertainty. The accuracy of existing correlations in literature can then also be evaluated using these results.

The purpose of this study was therefore to conduct heat transfer and pressure drop experiments in the quasi-turbulent and turbulent flow regimes and to develop an accurate heat transfer correlation that can be combined with recently developed laminar and transitional flow correlations, in order to obtain a single correlation that is valid for all flow regimes. The main objectives were: (1) To take accurate heat transfer and pressure drop measurements on a smooth tube in the quasi-turbulent and turbulent flow regimes and to quantify the uncertainties of the Reynolds numbers, Nusselt numbers and friction factors. The pressure drop data were not the focus of this study as these data were only used as complementary data to the heat transfer data. (2) To evaluate and compare the existing turbulent correlations in literature with these data. (3) To develop a new heat transfer correlation from this experimental data and compare it to existing correlations and experimental data from literature. (4) To link this work in the quasi-turbulent and turbulent flow regimes to recent work, with low uncertainties, conducted in the laminar and transitional flow regimes [43, 49, 57], by providing a single Nusselt number correlation that is valid for all flow regimes.

2. Experimental set-up and data logging

2.1 Experimental set-up

The experimental set-ups were housed in the Clean Energy Research Group laboratory at the University of Pretoria and is shown schematically in Fig. 2(a). The experimental set-ups and different test sections that were used have been described in detail in references [43, 49, 57-65] and will only be briefly discussed in this paper. The experimental set-up consisted of a closed-loop system, which circulated the test fluid from a storage tank, through the test section and back to the storage tank, using electronically controlled pumps. The storage tank was maintained at a preselected temperature (20 °C) because it was externally connected to a thermostat-controlled bath that cooled the heated fluid. The fluid in the storage tank was continuously pumped through a filtration cycle to remove any solid particles that might have entered the system, as well as to enhance mixing and prevent thermal stratification inside the storage tank.

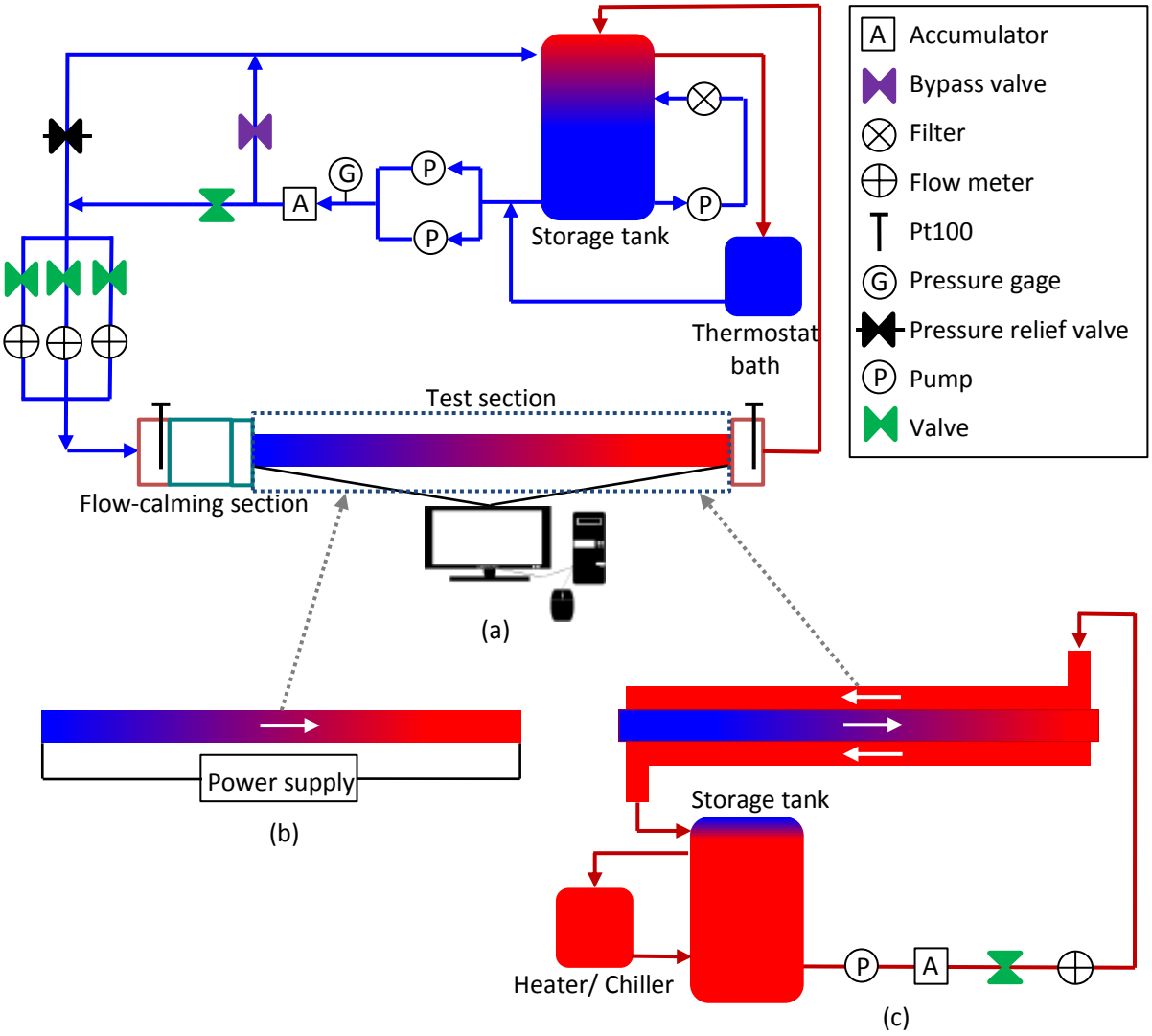

Fig. 2: Schematic representation of (a) the experimental set-up used to conduct heat transfer and pressure drop measurements, (b) the constant heat flux test section and (c) the constant surface temperature test section. Test sections (b) and (c) replace the test section in the dotted grey rectangle in (a).

A bladder accumulator was installed upstream of the flow meters and the test section to dampen possible pulsations from the pump. This ensured constant pressures and mass flow rates at the inlet of the test section. A bypass valve was inserted after the accumulator to allow a fraction of the test fluid to flow back to the storage tank. During the experiments, the supply valve was partially closed and the bypass valve partially opened, so that the pump was operated close to its maximum speed to ensure a preselected mass flow rate of test fluid to the test section. The increased pump speed, as well as the increase in pressure at the pump inlet (monitored using the pressure gauge), led to decreased mass flow rate pulsations [66]. The valve positions were adjusted throughout the experiments to minimise the flow pulsations for all the measurements. A pressure relief valve was used to allow the test fluid to flow directly to the storage tank if the pressure exceeded the preselected threshold.

Because the mass flow rates varied over a wide range, Coriolis mass flow meters with different flow rate capacities were installed in parallel. The mass flow meter that would produce the most accurate mass flow rate measurements was selected during the experiments. The mass flow rates were controlled by frequency drives, which were connected to the pump. The required mass flow rate was therefore obtained by increasing or decreasing the pump speed. Downstream of the mass flow meters, the fluid flowed through a flow-calming section to the test section and mixer, and then back into the storage tank.

Two different test section configurations were investigated in this study. The first configuration consisted of a single tube that was electrically heated to obtain a constant heat flux boundary condition and is schematically illustrated in Fig. 2(b). A test section in a counter-flow tube-in-tube configuration was also used. As schematically illustrated in Fig. 2(c), the counter-flow configuration was serviced with a hot water and a cold water stream. The inner tube of the heat exchanger was used as the test section and was serviced with cold water and the annulus was serviced with hot water when the test fluid was being heated. When the test fluid was being cooled, the test section was serviced with hot water and the annulus was serviced with cold water. The fluid in the annulus had a similar closed-loop system than for the test section.

2.2 Flow-calming section

A flow-calming section, similar to the one used by Ghajar [67-77], was installed upstream of the test section to straighten the flow. A bleed valve was installed prior to the inlet section to bleed air that entered the flow-calming section. The Pt100 probe connection inside the flow-calming section was used as another bleed valve. The flow-calming section was properly insulated against heat loss using Armaflex insulation with a thermal conductivity of 0.034 W/m.K. Peep holes and lids were incorporated into the insulation so that any air bubbles could be detected.

2.3 Test section

The test sections (Fig. 2(a)) covered a wide range of tube diameters and tube lengths and the details of the different test sections can be found in references [43, 49, 57-65]. T-type thermocouples were used to measure the surface temperatures at selected axial locations on the test sections. Depending on the test section configuration and heating method, the thermocouples were either soldered or glued onto the test sections. A 30 mm long capillary tube was silver soldered at each pressure tap station. To ensure that the pressure taps did not cause flow obstructions in the test section [78], a hole of less than 10% of the test section's inner diameter was drilled through the capillary tube and the tube wall. Care was taken to remove all the burrs from the inside of the test section and the test section was visually inspected using a borescope. A bush tap with a quick release coupling was fixed to the capillary tube, and nylon tubing was used to connect the pressure taps to the differential pressure transducers. The test sections were insulated with Armaflex insulation with a thermal conductivity of 0.034 W/m.K.

2.4 Mixer

To obtain a uniform outlet temperature, a mixer was inserted after the test section. The purpose of the mixer was twofold: to house the splitter plates to mix the water exiting the test section, as well as to house a Pt100 probe, which was used to measure the outlet temperature. The mixer design was based on work done by Bakker *et al.* [79], who investigated laminar flow in static mixers with helical splitter plates. The mixer consisted of four copper splitter plates with a length-to-width ratio of 1.5. The elements were positioned and soldered such that the leading edge of an element was perpendicular to the trailing edge of the next element. Every splitter plate repeatedly split the thermal boundary layers to ensure a uniform temperature gradient in the radial direction. The splitter plates were placed inside the acetal mixer, which directed the fluid to flow over and along the Pt100 probe after it has been mixed. This ensured that the entire Pt100 probe was exposed to the mixed fluid and also eliminated any stagnant recirculation zones. The mixer was insulated to prevent any heat loss, and air was bled from the mixer using the Pt100 probe connection to the mixer housing.

2.5 Control and data logging

The mass flow rate of the pump was controlled by frequency drives that were connected to a personal computer via a data acquisition system. The data acquisition system was used to record the data from the Pt100 probes (temperatures), thermocouples (temperatures), pressure transducers (pressure drops) and flow meters (mass flow rates). The data acquisition system consisted of a personal computer using National Instruments LabVIEW software as well as SCXI (Signal Conditioning eXtensions for Instrumentation) hardware, which included terminal blocks, analogue-to-digital converters and

multiplexers. The measured raw data were saved as .txt files, and Mathworks MATLAB scripts were in general used for the data processing.

3. Data reduction

Two different methods were used to obtain the surface temperatures: (1) direct temperature measurements (TM) using the thermocouples on the test section and (2) the Wilson plot/modified Briggs and Young method (WP) method [80-82]. The data reduction method used for the different test section configurations has been described in detail in references [43, 49, 57-65]. Therefore, only the data reduction method of the main parameters is given in this paper. The bulk fluid temperatures, T_b, were calculated as

$$T_b = \frac{T_i + T_o}{2} \tag{9}$$

The properties of the test fluid (density, ρ, dynamic viscosity, μ, thermal conductivity, k, specific heat, C_p, Prandtl number, Pr, and thermal expansion coefficient, β) were determined at the bulk fluid temperature.

The Reynolds numbers, Re, were calculated as

$$Re = \frac{\dot{m}D}{\mu A_c} \tag{10}$$

where $\dot{m}$ is the measured mass flow rate inside the tube, D the inner-tube diameter, μ the dynamic viscosity and A_c the cross-sectional area of the test section ($A_c = \pi/4D^2$).

After the Reynolds numbers and Nusselt numbers were calculated using either surface temperature measurements (Section 3.1) or the Wilson plot/modified Briggs and Young method (Section 3.2), the heat transfer results were also investigated in terms of the Colburn j-factors. This was to account for the variations in the Prandtl numbers of sequential measurements and to investigate the relationship between heat transfer and pressure drop:

$$j = \frac{Nu}{RePr^{\frac{1}{3}}} \tag{11}$$

The Graetz numbers, Gz, were determined as

$$Gz = RePr\frac{D}{x} \tag{12}$$

The friction factors, f, were calculated from the mass flow rate and pressure drop measurements, ΔP, between two pressure taps, which were apart from each other a length L:

$$f = \frac{2\Delta PD}{L\rho V^2} = \frac{\Delta P \rho D^5 \pi^2}{8\dot{m}^2 L} \tag{13}$$

In general in this paper, the percentage error of a measurement or calculated value was determined as %error = $|M_{exp} - M_{cor}|/M_{ref} \times 100$. When the experimental set-up and data reduction method were validated, M_{ref} was obtained from existing correlations in literature, M_{cor}. However, when the accuracies of the correlations were determined, M_{ref} was obtained from the experimental data, M_{exp}. The average percentage error was taken as the average of the absolute errors of the data points.

3.1 Surface temperature measurements (TM)

The average surface temperature, T_w, along a tube length, L, measured from the inlet of the test section, was calculated from the local surface temperatures, $T_w(x)$, using the trapezoidal rule:

$$T_w = \frac{1}{L}\int_0^L T_w(x)\, dx \tag{14}$$

The heat transfer coefficients, h, were determined from the following equation, because the heat flux, $\dot{q}$, surface temperature, T_w, and bulk fluid temperature, T_b, were known:

$$h = \frac{\dot{q}}{(T_w - T_b)} \tag{15}$$

The Nusselt numbers, Nu, were determined from the heat transfer coefficients as follows:

$$Nu = \frac{hD}{k} \tag{16}$$

The Grashof numbers, Gr, were determined as

$$Gr = \frac{g\beta(T_w - T_m)D^3}{\nu^2} \tag{17}$$

where 9.81 m/s^2 was used for the gravitational acceleration, g, and the kinematic viscosity was obtained from the density and dynamic viscosity ($\nu = \mu/\rho$).

3.2 Wilson plot method

The Reynolds numbers for the inner tube and annulus were calculated as follows:

$$Re_i = \frac{4\dot{m}_i}{\pi D_{ii}\mu_i} \tag{18}$$

$$Re_o = \frac{4\dot{m}_o}{\pi(D_{oi} - D_{io})\mu_o} \tag{19}$$

For the tube-in-tube test section configurations, the first subscript of the diameter, D, refers to the tube and the second subscript refers to the tube surface. For example, D_{oi} indicates the inner surface of the outer tube. By conducting a wide set of experiments at different mass flow rate measurements [60] for the inner stream, the Nusselt number correlations were determined as function of Reynolds number, Prandtl number and viscosity ratio in the format of the Sieder and Tate equations (Eqs. (20) and (21)) by using the modified Wilson plot method as prescribed by Briggs and Young [80].

$$Nu_i = C_i Re_i^{P_i} Pr_i^{\frac{1}{3}} \left(\frac{\mu_i}{\mu_w}\right)^{0.14} \tag{20}$$

$$Nu_o = C_o Re_o^{P_o} Pr_o^{\frac{1}{3}} \left(\frac{\mu_o}{\mu_w}\right)^{0.14} \tag{21}$$

4. Uncertainty analysis

The method proposed by Dunn [83] was used to calculate the uncertainties of the parameters obtained in the data reduction. All uncertainties were calculated within the 95% confidence interval. The details of the uncertainty analysis method can be found in references [43, 49, 57-65] and the results are summarised in Table 3. The Wilson Plot uncertainties were much more challenging than that of the surface temperature uncertainties, because the linear regression analysis used in the Wilson Plot method had to be incorporated. The details of the Wilson Plot uncertainty calculations are given in Coetzee [60].

Table 3: Reynolds number, Nusselt number and friction factor uncertainties of the quasi-turbulent and turbulent experimental data of this study. The uncertainties of the recent work conducted in the laminar and transitional flow regimes are summarised in Meyer and Everts [57].

Reference	Fluid	D [m]	L [m]	BC	Heating/ Cooling	δRe [%]	δNu [%]	δf [%]
Grote [59]	Water	0.0052	1.0	$\dot{q}$	Heating	1.1	2.5 – 3.2	2.0 – 5.0
	MWCNT					1.3 – 1.7	2.5 – 3.2	2.0 – 5.0
Coetzee [60]	Water	0.0083	3.75	Ts	Cooling	1.0	2.1	0.6 – 4.5
		0.0144				1.0	1.6	0.6 – 4.5
Steyn [58]	Water	0.0084	5.08	Ts	Cooling	2.6 – 2.7	2.1 – 2.6	11.9 – 12.2
		0.0145		Ts	Cooling	1.7 – 1.8	2.1 – 4.0	7.0 – 8.8
		0.0145		Ts	Heating	1.7 – 1.9	2.1 – 4.7	7.0 – 10.8
Everts [61]	Water	0.0115	9.5	$\dot{q}$	Heating	1.1	3.3- 16.7	1.0 – 2.9
		0.004	5.49			1.5	4.9 – 23.7	9.3 – 9.4
Abolarin [62]	Water	0.019	4.8	$\dot{q}$	Heating	0.3 – 0.4	2.1 – 5.7	0.6 – 3.5
Bashir [65]	Water	0.0051	4.52	$\dot{q}$	Heating	1.0 – 1.1	3.4 – 8.9	2.0 – 3.8

Table 3 indicates that the Reynolds numbers uncertainty was less than 3% for all the experimental data. The Nusselt number uncertainties of the studies that specifically focussed on the turbulent flow regime [58, 60] were less than 5%. The other studies [59, 61, 62, 65] that focussed more on the laminar

and transitional flow regimes, but also included limited experiments in the turbulent flow regime had higher Nusselt number uncertainties (with specific reference to Everts [61]). The maximum friction factor uncertainties in the different test sections varied between 3% and 12%. The uncertainties of the recent work conducted in the laminar and transitional flow regimes are summarised in Meyer and Everts [57]. For laminar forced convection uncertainties were less than 10%, while the laminar mixed convection uncertainties were less than 5%. The Nusselt number uncertainties increased to approximately 10% in the transitional flow regime. The transitional flow uncertainties were in general higher than in the other flow regimes owing to the mass flow rate and temperature fluctuations that occurred in this flow regime [43].

5. Experimental procedure

The general experimental procedure is briefly discussed in this paper and more details are given in Everts [61] and Coetzee [60] for the constant heat flux ($\dot{q}$) and constant surface temperature (Ts) test section configurations respectively, as shown schematically in Fig. 2(b) and (c). Wilson-plot experiments were usually operated with the annulus Reynolds numbers much higher than the Reynolds numbers in the inner tube, because this provided accurate results. The regression method only indirectly produced one average temperature and not a series of temperature measurements in an axial direction, as with the constant heat flux method. Therefore, during these conditions the surface temperature of the inner tube was constant, or assumed to be constant.

Steady-state conditions were reached approximately one hour after the start-up of the experimental set-up. Steady-state conditions were assumed once there was no increase or decrease in temperatures, pressure drops, and mass flow rates within a period of approximately two minutes. Different time periods were considered and a period of approximately two minutes was found to be sufficient. After steady state had been reached, 200 measuring points (temperature, pressure and mass flow rate) were captured at a frequency of 10 Hz. The average value of the 200 measuring points was then used as one data point in the calculations. As the mass flow rate was increased with a very small increment to the next Reynolds number, the time required to reach steady-state between Reynolds number increments reduced to approximately 15 min in the quasi-turbulent and turbulent flow regimes. However, the time required to reach steady state depended on the mass flow rate inside the test section [61]. In the laminar flow regime, at very low Reynolds numbers, approximately 30 min was required to reach steady-state conditions. As the mass flow rate was increased, the time required for steady state decreased to 20 min. Although the mass flow rates in the transitional flow regime were greater than in the laminar flow regime, up to one hour was required to reach steady state owing to the mass flow rate and temperature fluctuations inside the tube. The Reynolds number was increased by increasing the mass flow rate using the frequency drives connected to the pumps. The supply and bypass valves were continuously adjusted to ensure that the pumps operated close to their maximum speeds, to reduce mass flow rate pulsations.

Table 4: Experimental test matrix of this study. *Ts* refers to a constant surface temperature boundary condition and $\dot{q}$ to a constant heat flux boundary condition.

Author	Fluid	Data points	Reynolds number	Prandtl number	Boundary condition	Heating/ cooling	Diameter [mm]	Length [m]
Grote [59]	Water	140	2 656 – 8 356	6.30 – 7.20	$\dot{q}$	Heating	5.2	1.0
	MWCNT	85	2 445 – 7 029	7.57 – 9.97				
Coetzee [60]	Water	60	11 905 – 209 485	3.16 – 3.88	*Ts*	Cooling	8.3	3.75
		63	10 492 – 218 234	3.32 – 3.98			14.4	
Steyn [58]	Water	77	10 679 – 120 056	3.29 – 4.42	*Ts*	Cooling	8.4	5.08
		135	11 163 – 220 818	3.08 – 6.47	*Ts*	Cooling	14.5	
		62	10 880 – 91 680	3.91 – 8.42	*Ts*	Heating		
Everts [61]	Water	190	2 859 – 10 090	6.09 – 6.81	$\dot{q}$	Heating	11.5	9.5
		143	2 609 – 8 554	4.22 – 6.11			4.0	5.49
Abolarin [62]	Water	156	3 225 – 11 283	5.25 – 6.58	$\dot{q}$	Heating	19.0	4.8
Bashir [65]	Water	69	2 781 – 7 257	4.66 – 5.90	$\dot{q}$	Heating	5.1	4.52
Total		**1 180**	**2 445 – 220 818**	**3.08 – 9.97**				

Table 5: Experimental data in literature (2007 - 2016). *Ts* refers to a constant surface temperature boundary condition and $\dot{q}$ to a constant heat flux boundary condition.

Author	Fluid	Data points	Reynolds number	Prandtl number	Testing condition	Heating/ cooling	Diameter [mm]	Length [m]
Li *et al.* [84]	#22 lubricating oil	22	7 188 – 19 057	65.0 – 71.4	*Ts*	Cooling	17.0	2.0
Eiamsa-Ard *et al.* [85]	Air	6	4 614 – 19 451	0.47 – 0.65	$\dot{q}$	Heating	4.8	1.5
Buyukalaca *et al.* [86]	Air	15	3 099 – 22 209	0.47 – 0.72	$\dot{q}$	Heating	5.6	3.0
Bertsche *et al.* [87]	Water-glycol	18	3 319 – 22 585	7	*Ts*	Cooling	2.6	0.22
		7	4 041 – 17 747	10				
		12	3 179 – 13 497	13				
		11	3 457 – 12 420	16				
Total		**91**	**3 099 – 22 585**	**0.47 – 71.4**				

Table 6: Experimental data in literature (1913 - 1964). *Ts* refers to a constant surface temperature boundary condition and $\dot{q}$ to a constant heat flux boundary condition.

Author	Fluid	Data points	Reynolds number	Prandtl number	Testing condition	Heating/ cooling	Diameter [mm]	Length [m]
Webster [39]	Water	94	4 256 – 51 059	3.71 – 8.77	*Ts*	Heating	12.7	0.76
Morris & Whitman [3]	Water	12	10 107 – 38 816	2.83 – 3.15	*Ts*	Heating	15.7	0.27
	Gas oil	11	3 708 – 30 011	32.8 – 41.4				
	Straw oil	13	3 820 – 13 145	57.7 – 133				
	Light motor oil	2	3 212 – 4 303	203 – 276				

	Gas oil	15	3 634 – 44 149	18.1 – 31.2		Cooling		
	Straw oil	23	3 038 – 45 265	8.58 – 99.3				
	Light motor oil	6	4 265 – 9 363	87.0 – 164				
Clapp & FitzSimons [20]	Water	7	13 307 – 60 147	1.74 – 6.36	*Ts*	Heating	12.5	1.42
	Velocite B	10	3 100 – 7 094	72.1 – 76.4				
	Water	5	19 098 – 59 651	1.91 – 4.98		Cooling		1.33
	Velocite B	13	3 113 – 7 218	71.1 – 97.5				
Lawrence & Sherwood [23]	Water	32	4 746 – 132 530	2.16 – 7.44	*Ts*	Heating	15.1	3.38
		30	5 375 – 140 005	2.16 – 8.18				2.75
		31	6 868 – 98 034	2.32 – 8.34				1.84
		34	4 113 – 97 366	2.83 – 8.87				0.89
Sherwood & Petrie [16]	Water	131	3 050 – 113 000	1.94 – 3.91	*Ts*	Heating	12.5	1.22
	Acetone	54	3 730 – 89 500	3.69 – 4.45				
	Benzene	65	3 500 – 86 700	6.37 – 8.17				
	Kerosene	52	3 430 – 31 800	10.4 – 24.2				
	n-Butyl Alcohol	24	4 280 – 32 500	19.4 – 35.1				
Sherwood *et al*. [17]	Light hydrocarbon oil	26	3 130 – 5 570	102 – 130	*Ts*	Heating	15.1	3.53
		24	3 100 – 5 260	110 – 115				2.74
		14	3 050 – 4 930	132 – 141				1.83
		5	3 000 – 3 480	172 – 174				0.91
Barnes & Jackson [88]	Air	84	4 200 – 130 000	0.72	$\dot{q}$	Heating	6.3	0.30
	Helium	69	4 000 – 65 000	0.67				
	Carbon dioxide	28	8 000 – 40 000	0.75				
Stone *et al*. [32]	*n*-Hexadecane	24	12 500 – 223 800	11.6 – 18.6	$\dot{q}$	Heating	7.9	0.61
	Di(2-ethylhexyl) adipate	14	13500 – 124 200	15.1 – 24.2			7.9	
	Biphenyl	13	56 200 – 401 600	4.1 – 6.4			7.9	
		6	57 400 – 163 800	4.1 – 4.2			7.8	
		8	31 500 – 164 900	4.2 – 6.3			7.8	
	Monoisopropylbiphenyl	27	18 500 – 349 800	5.1 – 15.5			7.8	
McEligot [89]	Air	11	3 406 – 192 271	0.68 – 0.71	$\dot{q}$	Heating	3.1	0.51
	Helium	3	9 628 – 56 347	0.66				
Allen & Eckert [29]	Water	36	13 000 – 111 000	7.94	$\dot{q}$	Heating	19.1	0.57
Total		**1056**	**3 000 – 401 600**	**0.66 – 276**				

6. Experimental test matrix

Table 4 summarises the experiments that were conducted using the different test sections and testing conditions. The test matrix consisted of 1 180 Nusselt number and friction factor data points as a function of Reynolds number and Prandtl number. This covered a wide Reynolds number range of 2 445 – 220 818 and a narrower Prandtl number range of 3 – 10. Because the maximum Prandtl numbers of the experimental data of this study were limited to approximately 10, high Prandtl number experimental data from literature were used to evaluate the performance of the turbulent correlation developed in this study when high Prandtl number fluids are used.

The more recent experimental data used from literature between 2007 and 2016 are summarised in Table 5 and the much older experimental data used from literature between 1913 and 1964 are summarised in Table 6. The experimental databases obtained from literature made available to this study an additional 1 147 data points. The total number of Nusselt numbers that was used in Section 8 was thus 2 327. This is a much larger database than was used in previous studies. Although the uncertainties of the 1 180 data points generated by us for this study were known, the uncertainties of the 1 147 data points from literature were unfortunately unknown. Recent experimental data in the laminar and transitional flow regimes were used complimentary to the quasi-turbulent and turbulent experimental data of this study, to obtain a single Nusselt number correlation that is valid for all flow regimes. The test matrix is summarised in Meyer and Everts [57] and consisted of 1 046 mass flow rate measurements, 89 459 temperature measurements and 2 906 pressure drop measurements.

7. Validation

7.1 Friction factors

Fig. 3 compares the quasi-turbulent and turbulent friction factors predicted using the correlations of Petukhov [40], Blasius [90], Filonenko [91] and Fang *et al*. [92], which are the most prominent friction factor correlations in literature, with the experimental pressure drop data of this study. The performance of the experimental data compared with the correlations are summarised in Table 7. The results correlated very well with the Blasius [90] correlation with an average deviation of only 1.4% and all the data were predicted within 5%. Table 7 also indicates that experimental friction factors correlated very well with the correlations of Filonenko [91] and Fang *et al*. [92], with more than 90% of the data within 5% of the correlations and an average deviation of less than 2%. It can therefore be concluded from the experimental results that the existing friction factor correlations are adequate and very accurate and that further research on this topic is unnecessary. However, it was necessary to conduct pressure drop experiments in this study, because the friction factors were required in Section 8.1.

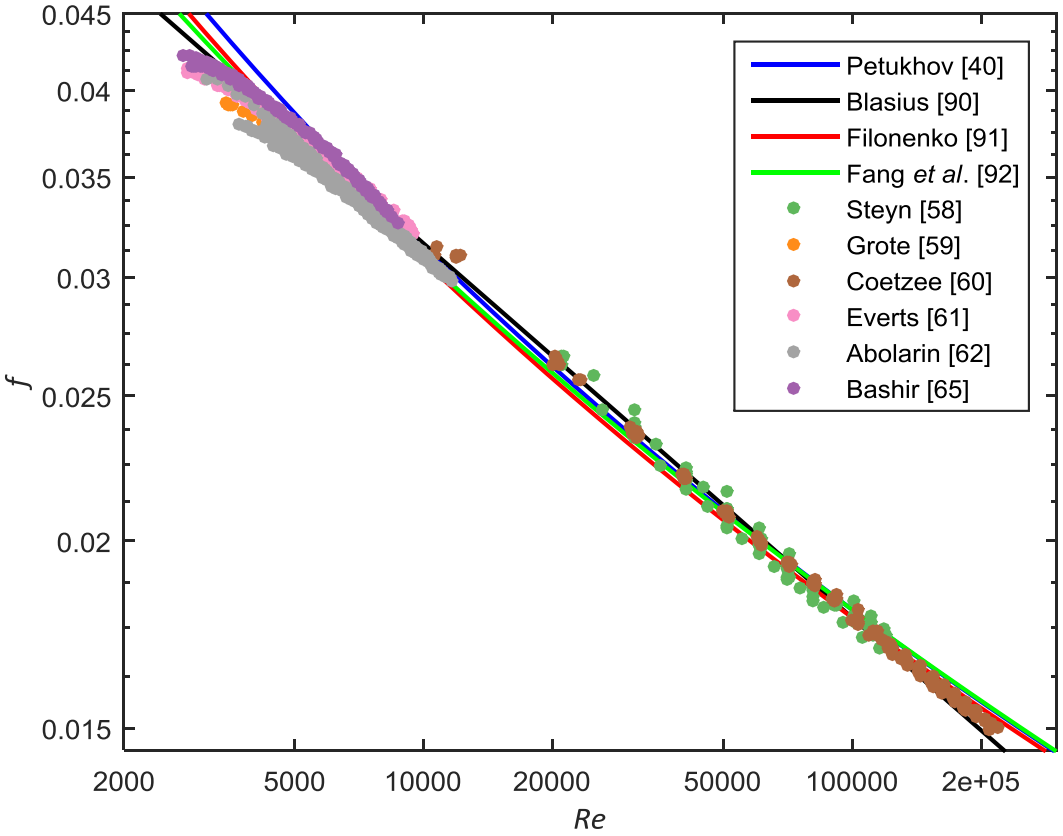

Fig. 3: Comparison of the quasi-turbulent and turbulent experimental pressure drop data of this study with the friction factors predicted using the correlations of Petukhov [40], Blasius [90], Filonenko [91] and Fang *et al.* [92].

Table 7: Performance of the experimental data of this study compared with the most prominent friction factor correlations in literature.

	Eq.	Range	Error ±5% [%]	Error ±10% [%]	Error Ave [%]
Blasius [90] $f = 0.3125Re^{-0.25}$	(22)	$4\times10^3 < Re < 10^5$	100	100	1.4
Petukhov [40] $f = (0.79\ln Re - 1.64)^{-2}$	(23)	$3\times10^3 < Re < 5\times10^6$	78	99	3.1
Filonenko [91] $f = (1.8\log Re - 1.5)^{-2}$	(24)	$3\times10^3 < Re < 10^6$	92	100	2.0
Fang *et al.* [92] $f = 0.25\left[\left(\log\frac{150.39}{Re^{0.98865}}\right) - \frac{152.66}{Re}\right]^{-2}$	(25)	$3\times10^3 < Re < 10^8$	96	100	1.7

7.2 Heat transfer coefficients

Fig. 4 compares the Nusselt numbers obtained using direct surface temperature measurements (TM) [58] with the Nusselt numbers obtained using the Wilson plot method (WP) [60]. Both data sets were obtained in test sections with an inner diameter of 14.2 mm and the fluid was cooled in a test section with a relatively constant surface temperature (T_s) boundary condition (Fig. 2(c)), thus the Prandtl numbers were approximately the same.

Fig. 4 indicates that the Nusselt numbers of the two data sets correlated very well with a maximum deviation of only 6%. Therefore, in this paper, both methods generated accurate surface temperatures,

and thus heat transfer coefficients. Furthermore, these two data sets were compared with the Nusselt numbers obtained using direct surface temperature measurements in a test section (D_i = 19 mm) with a constant heat flux ($\dot{q}$) boundary condition [62]. The results correlated very well with a maximum deviation of 8%, which confirms that the heat transfer coefficients in the turbulent flow regime are independent of the boundary condition. The validation of the heat transfer coefficients are given in Section 8.2 where the prominent turbulent heat transfer correlations in literature are compared and evaluated.

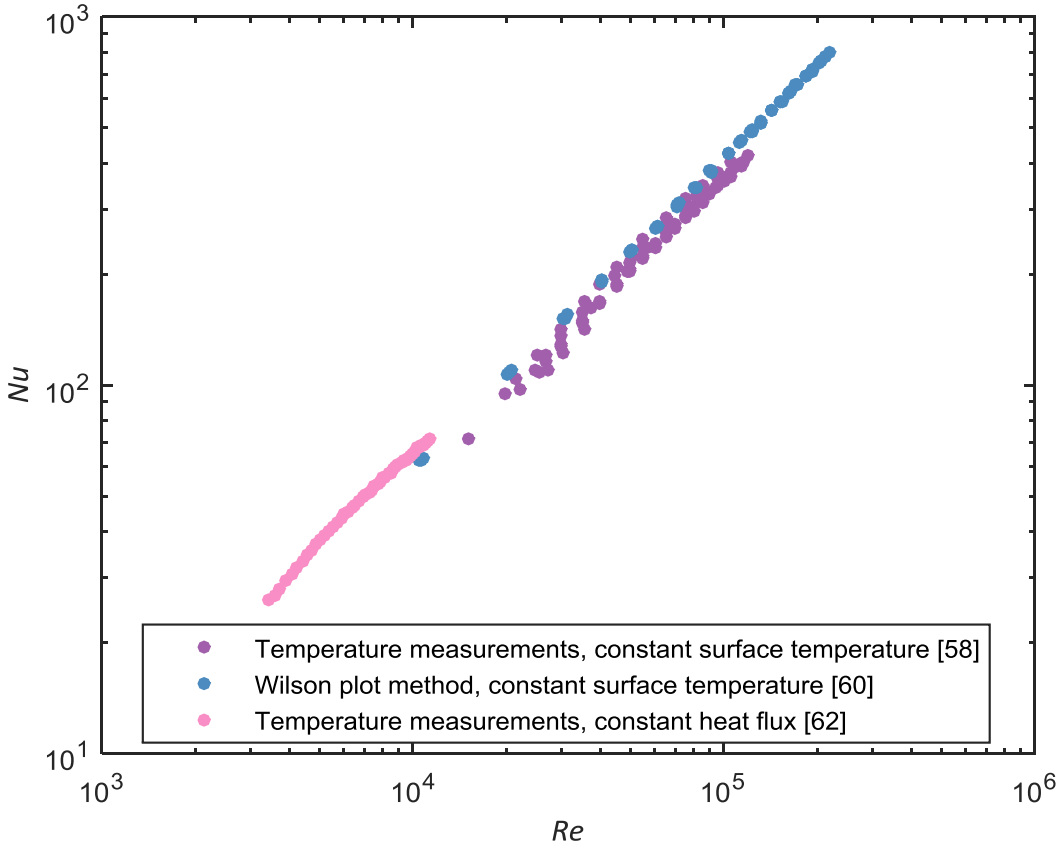

Fig. 4: Comparison of the Nusselt numbers obtained using direct surface temperature measurements and the Wilson plot method for both constant surface temperature and constant heat flux boundary conditions.

8. Results

8.1 Relationship between heat transfer and pressure drop

Fig. 5 compares the Colburn *j*-factors and the friction factors as a function of Reynolds number and the trends of these two parameters were similar (it should be noted that a log-log scale was used). This is as expected because the Chilton-Colburn analogy [40], which was developed for laminar and turbulent flow over flat plates, determined that the relationship between friction factor (pressure drop) and Colburn *j*-factor (heat transfer) was directly proportional. Everts and Meyer [49] investigated the relationship between pressure drop and heat transfer in smooth tubes in all flow regimes and found that

a direct relationship between heat transfer and pressure drop existed not only in the laminar and turbulent flow regimes, but also in the transitional and quasi-turbulent flow regimes.

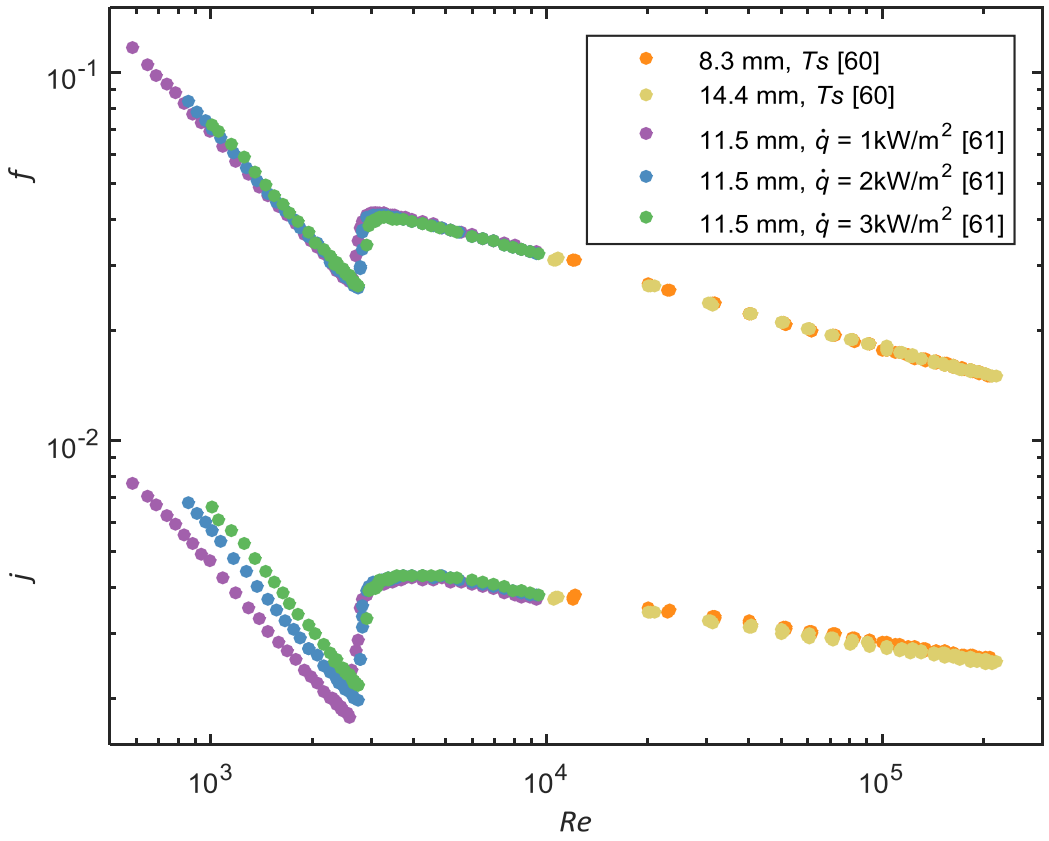

Fig. 5: Comparison of the pressure drop and heat transfer results in terms of the friction factors and Colburn *j*-factors as a function of Reynolds number.

To quantitatively investigate the relationship between pressure drop and heat transfer, *f*/*j*-factors were obtained by dividing the friction factors by the Colburn *j*-factors (Fig. 6). It is desirable to know this relationship between heat transfer and pressure drop, because it makes it possible to determine either the heat transfer coefficients or the friction factors when the other variable is known. Everts and Meyer [49] concluded that the relationship between heat transfer and pressure drop is a strong function of Grashof number in the laminar flow regime, while it is a strong function of Reynolds number in the other three flow regimes.

A power curve-fit through the *f*/*j*-factors between Reynolds numbers of 3 000 (quasi-turbulent) and 220 000 (turbulent) in Fig. 6 was performed to quantify the relationship between heat transfer and pressure drop in the quasi-turbulent and turbulent flow regimes as

$$\frac{f}{j} = 24.475 Re^{-0.117} \tag{26}$$

By substituting the Colburn *j*-factor with Eq. (11), the following correlation was obtained to calculate the Nusselt numbers as a function of friction factor:

$$Nu = 0.041Re^{1.117}Pr^{1/3}f \tag{27}$$

Therefore, Eq. (27) makes it possible to calculate the Nusselt numbers when the Reynolds number, Prandtl number and friction factor are known. In the case when friction factor data are not available, the friction factor in Eq. (27) can be substituted by the correlation of Blasius ($f = 0.3125Re^{-0.25}$) for a smooth tube, because it is shown in Table 7 that this correlation was able to predict the friction factors of this study with an average deviation of 1.4%. The resulting correlation (without explicitly the friction factor) is then:

$$Nu = 0.013Re^{0.867}Pr^{1/3} \tag{28}$$

Eq. (28) performed very well and was able to predict 79% of the experimental data of this study within errors of 10% and 96% of the data points within 20% errors. The average deviation was 6.4%. Furthermore, Eq. (28) was able to predict 34% of the experimental data from literature [3, 16, 17, 20, 23, 29, 39, 84-89] within errors of 10% and 63% of the data points within 20% errors.

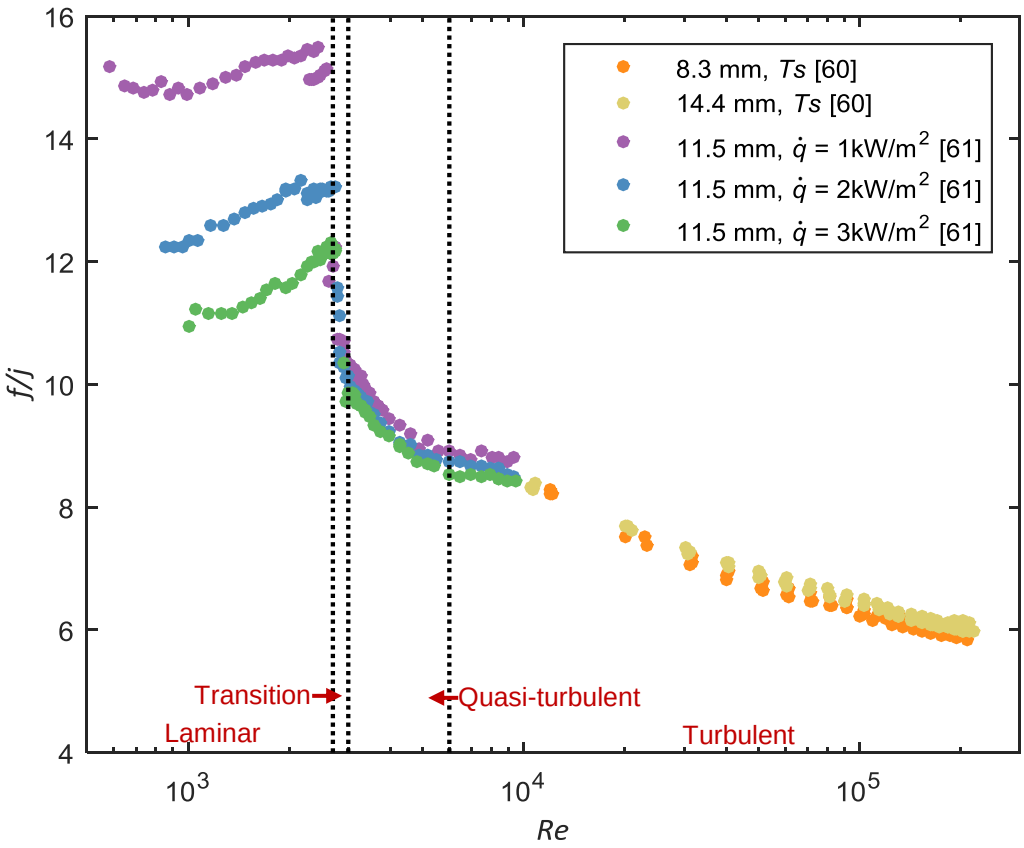

Fig. 6: Comparison of the friction factors divided by the Colburn *j*-factors as a function of Reynolds number.

It should also be noted from the very strong relationship between friction factors and Colburn *j*-factors (as was shown by Everts and Meyer [49] and Meyer and Abolarin [62]), that it can be postulated that Eq. (27) can be considered as a general relationship that will not only be valid for the smooth tubes of this study, but also for rough tubes. Thus, if the friction factor in Eq. (27) of a rough tube can be

determined from the Moody chart [40], correlations, or from experiments, then it should be possible to directly estimate the Nusselt number from Eq. (27) without additional experiments or from developing additional correlations, tables or graphs.

8.2 Evaluation of existing correlations

The existing correlations in literature were evaluated using the experimental data of this study (Fig. 7) as well as experimental data from literature [3, 16, 17, 20, 23, 29, 39, 84-89] (Fig. 8). Table 1 indicates that the correlations are functions of fluid properties, such as Prandtl number and viscosity, and test section dimensions. The consequence is that a single correlation produced several 'lines' for different Prandtl numbers when plotted in terms of Nusselt number as a function of Reynolds number. It was therefore not feasible to compare the different correlations in terms of the Nusselt numbers as a function of Reynolds number in a single graph, but rather to compare the experimental Nusselt numbers to the Nusselt numbers obtained using the different correlations. Table 8 summarises the ranges of the correlations, as well as the performance of the correlations compared with the experimental data of this study and literature.

The black dotted ovals A, C, and D in Fig. 7 indicate that the correlations of Dittus and Boelter [2], Sieder and Tate [19], and Hausen [1] could not accurately predict the lower Nusselt numbers which fell in the quasi-turbulent flow regime. Although Table 8 indicates that the correlation of Colburn [9] was able to predict almost all the data of this study within 20% and with an average deviation of only 7%, the black dotted circle, B, in Fig. 7(b) indicates that the results began to deviate at lower Nusselt numbers, thus lower Reynolds numbers in the quasi-turbulent flow regime. Fig. 7(e) and (f) indicate that the correlations of Petukhov [26] and Gnielinski [31] were able to accurately predict the majority of the Nusselt numbers in the quasi-turbulent flow regime and the average deviation of both correlations was approximately 8%. The correlation of Gnielinski [31] performed slightly better than the correlation of Petukhov [26], because it was able to predict 92% of the experimental data of this study within 20%. It should be noted that although the average deviation between the experimental data of this study and the correlation of Gnielinski [31] was 8%, only 70% of the data were predicted within 10%.

Table 8: Performance of existing Nusselt number correlations compared with the experimental data of this study and literature [3, 16, 17, 20, 23, 29, 32, 39, 84-89].

	Eq.	Error					
		This study			Literature [3, 16, 17, 20, 23, 29, 32, 39, 84-89]		
		±10%	±20%	Ave%	±10%	±20%	Ave%
Dittus and Boelter [2]	(2)	38	76	14	40	70	17
Colburn [9]	(3)	74	99	7.0	25	57	19
Sieder and Tate [19]	(4)	27	68	17	39	61	19
Hausen [1]	(5)	38	89	12	44	76	14
Petukhov [26]	(6)	72	89	8.5	54	79	13
Gnielinski [31]	(7)	70	92	8.0	47	76	15
Range		2 445 < *Re* < 220 818 3 < *Pr* < 10			3 000 < *Re* < 401 600 0.47 < *Pr* < 273		

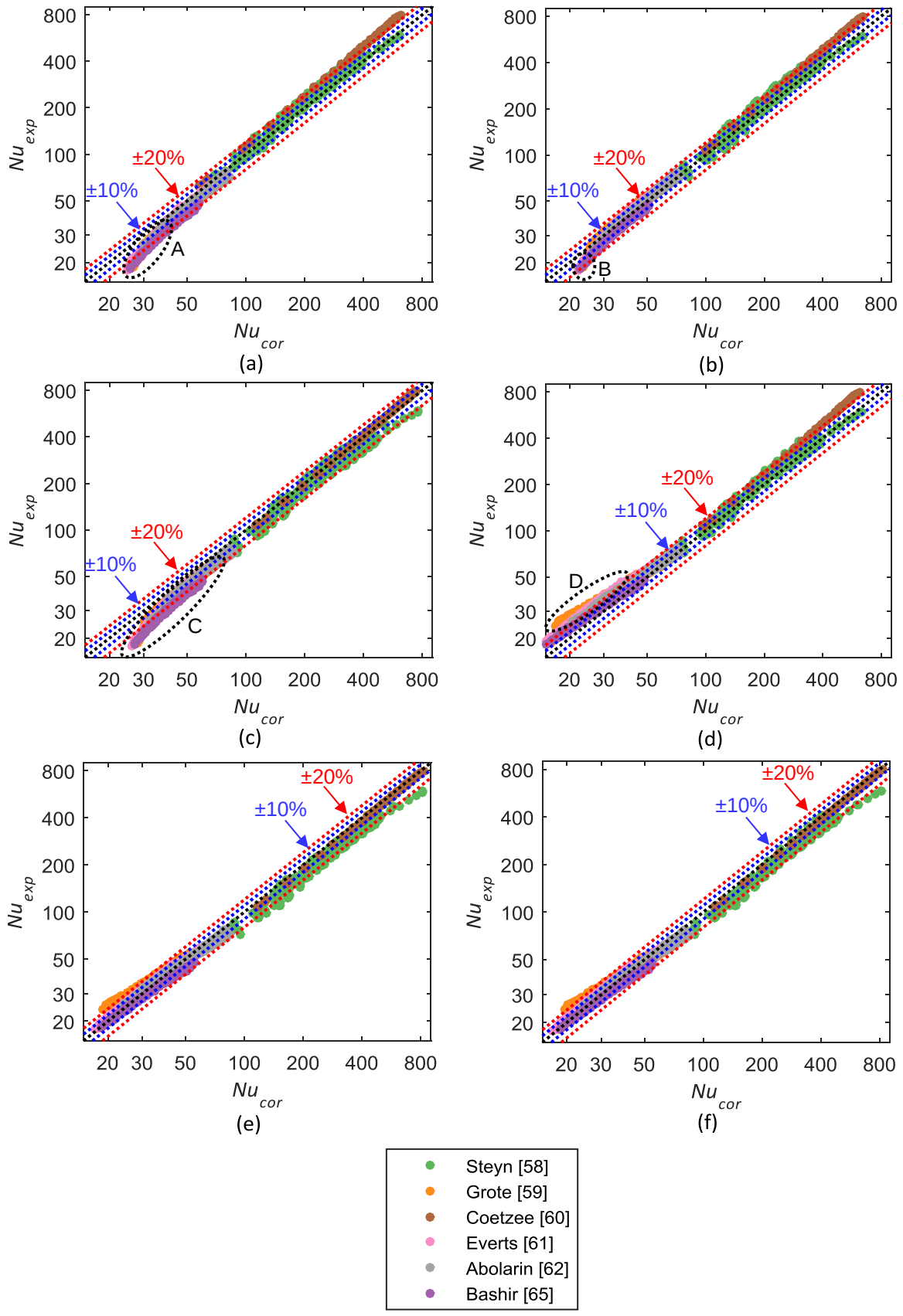

Fig. 7: Comparison of the experimental heat transfer data of this study with the Nusselt numbers predicted using the correlations of (a) Dittus and Boelter [2], (b) Colburn [9], (c) Sieder and Tate [19], (d) Hausen [1], (e) Petukhov [26] and (f) Gnielinski [31].

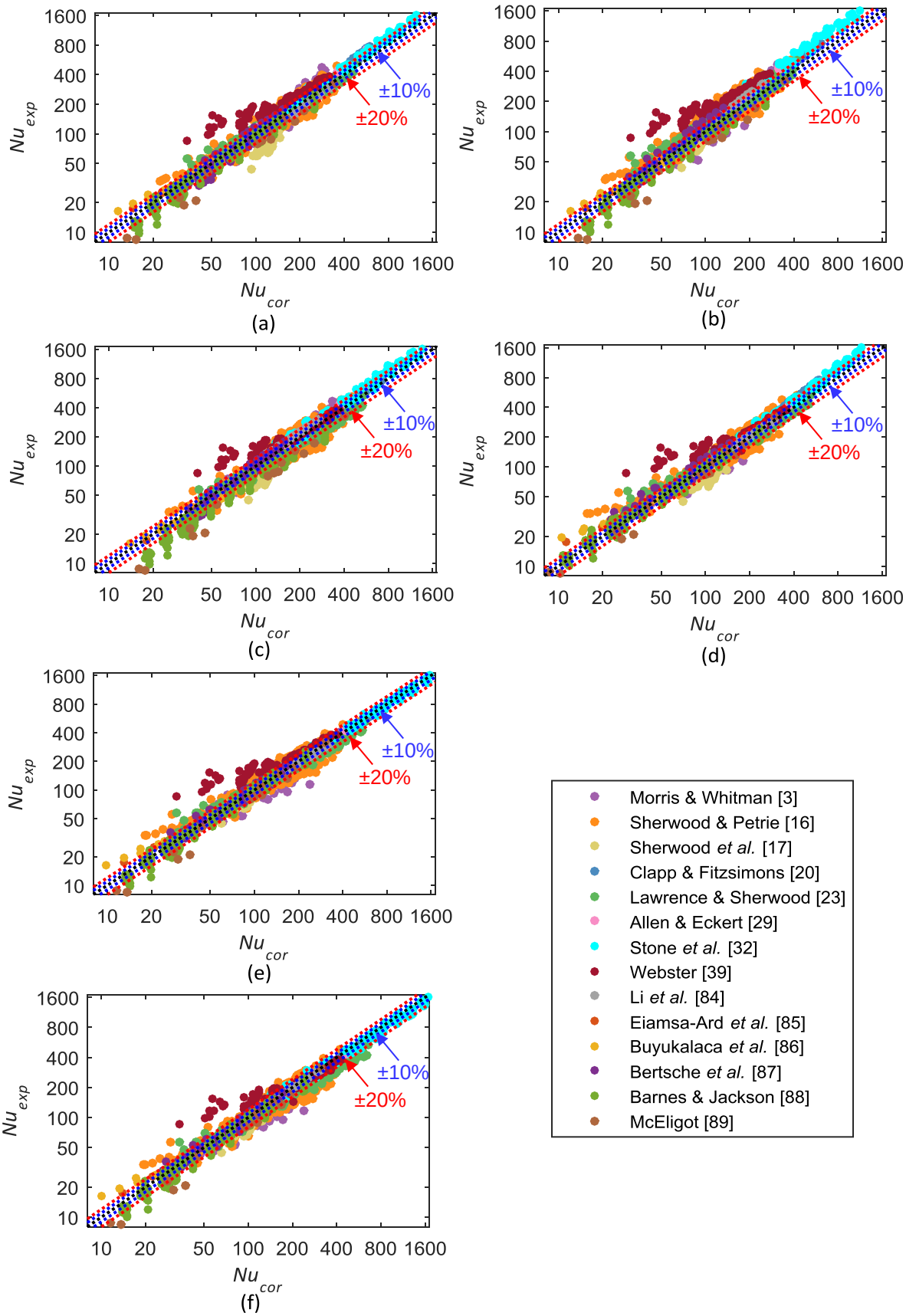

Fig. 8: Comparison of the experimental heat transfer data in literature [3, 16, 17, 20, 23, 29, 32, 39, 84-89] with the Nusselt numbers predicted using the correlations of (a) Dittus and Boelter [2], (b) Colburn [9], (c) Sieder and Tate [19], (d) Hausen [1], (e) Petukhov [26] and (f) Gnielinski [44].

Comparing the experimental data of this study in Fig. 7 with the experimental data from literature [3, 16, 17, 20, 23, 29, 39, 84-89] in Fig. 8, significant scatter can be observed in Fig. 8. This is as expected, because the experiments were conducted across a period of more than 100 years using a wide range of tube diameters, tube lengths, test fluids, heating or cooling methods, as well as measuring instrumentation. Unfortunately, the uncertainties of these experimental heat transfer results are not available, because the art of uncertainty analyses was not established as a requirement for the publication of experimental data in scholarly journals. Table 8 indicates that the correlations of Hausen [1], Petukhov [26], and Gnielinski [31] gave the best results and were able to predict more than 70% of the data within 20%. Although the Reynolds number range of the correlation of Gnielinski [31] was wider, the overall performance of the correlation of Petukhov [26] was slightly better.

8.3 New Nusselt number correlations

A new Nusselt number correlation for quasi-turbulent and turbulent flow is presented in Section 8.3.1, while a Nusselt number correlation for transitional flow is presented in Section 8.3.2. In Section 8.3.3, a single correlation that can be used for laminar, transitional, quasi-turbulent and turbulent flow is presented. Section 8.3.4 gives a summary of the correlations presented in this paper.

8.3.1 Quasi-turbulent and turbulent flow

Fig. 9 compares the experimental heat transfer data of this study in terms of the Nusselt number, as a function of Reynolds number. This figure indicates that the Nusselt numbers increased with increasing Reynolds number, as can be expected; however, the Nusselt numbers did not form a single diagonal line and scatter existed. This is because the Prandtl numbers of the different experimental data points varied and, as summarised in Table 4, the experiments were conducted in test sections with a wide range of diameters and lengths, at different heat fluxes, using different test fluids, heating methods and boundary conditions.

Friend and Metzner [93] found that for turbulent flow with fluids with Prandtl numbers between 0.46 and 346, the effect of Prandtl number can be accounted for by using an exponent of 0.42 for the Prandtl number instead of an exponent value of 1/3. Furthermore, Gnielinski [31] introduced the Prandtl number ratio, $(Pr/Pr_w)^{0.11}$, to account for the variable fluid properties across the cross-section. Therefore, to account for different Prandtl numbers (due to the different fluid temperatures and test fluids), as well as variable fluid properties across the test section, Fig. 10 compares the heat transfer results in terms of $Nu/[Pr^{0.42}(Pr/Pr_w)^{0.11}]$ as a function of Reynolds number. This figure indicates that the Prandtl number correction, $Pr^{0.42}(Pr/Pr_w)^{0.11}$, was sufficient because the scatter due to the different test sections and operating conditions in Fig. 9, reduced significantly in Fig. 10. The dotted circle in Fig. 10 indicates that the results began to deviate at Reynolds numbers greater than 130 000. The decreasing temperature differences with increasing mass flow rates, led to higher uncertainties at very high Reynolds numbers.

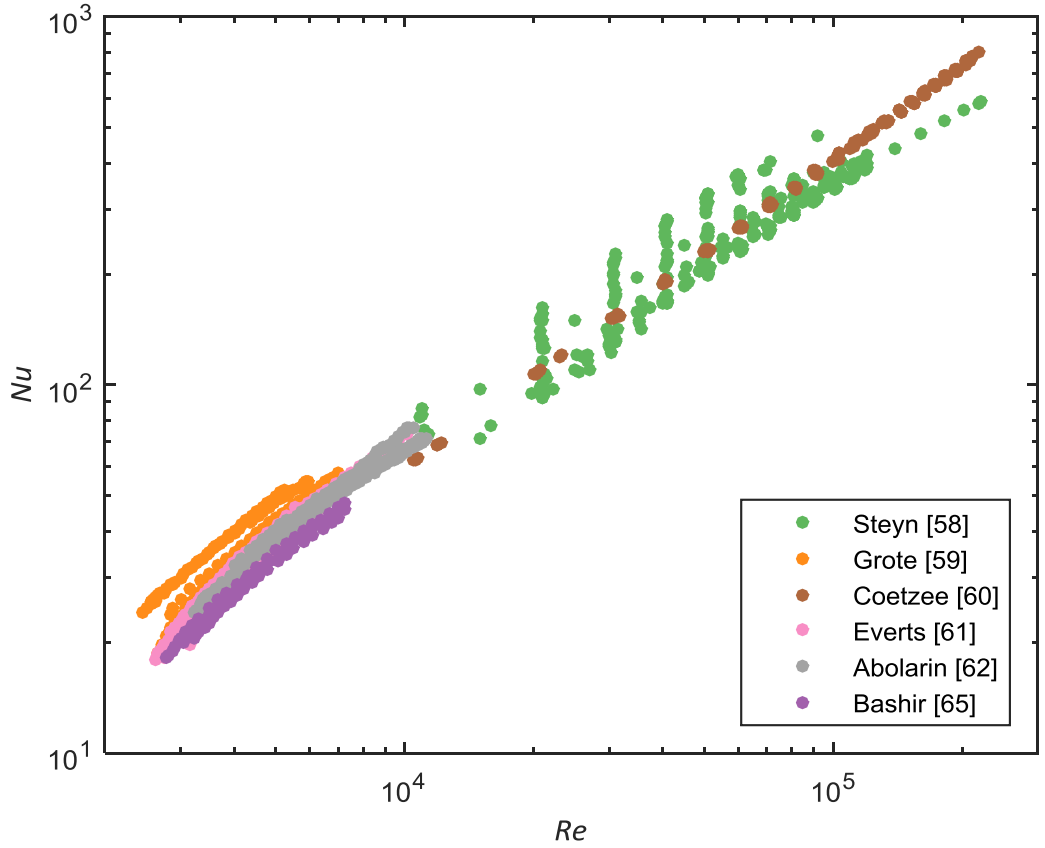

Fig. 9: Comparison of the experimental heat transfer data of this study (obtained using different heat fluxes, heating methods, test fluids and test sections) in terms of the Nusselt number as a function of Reynolds number.

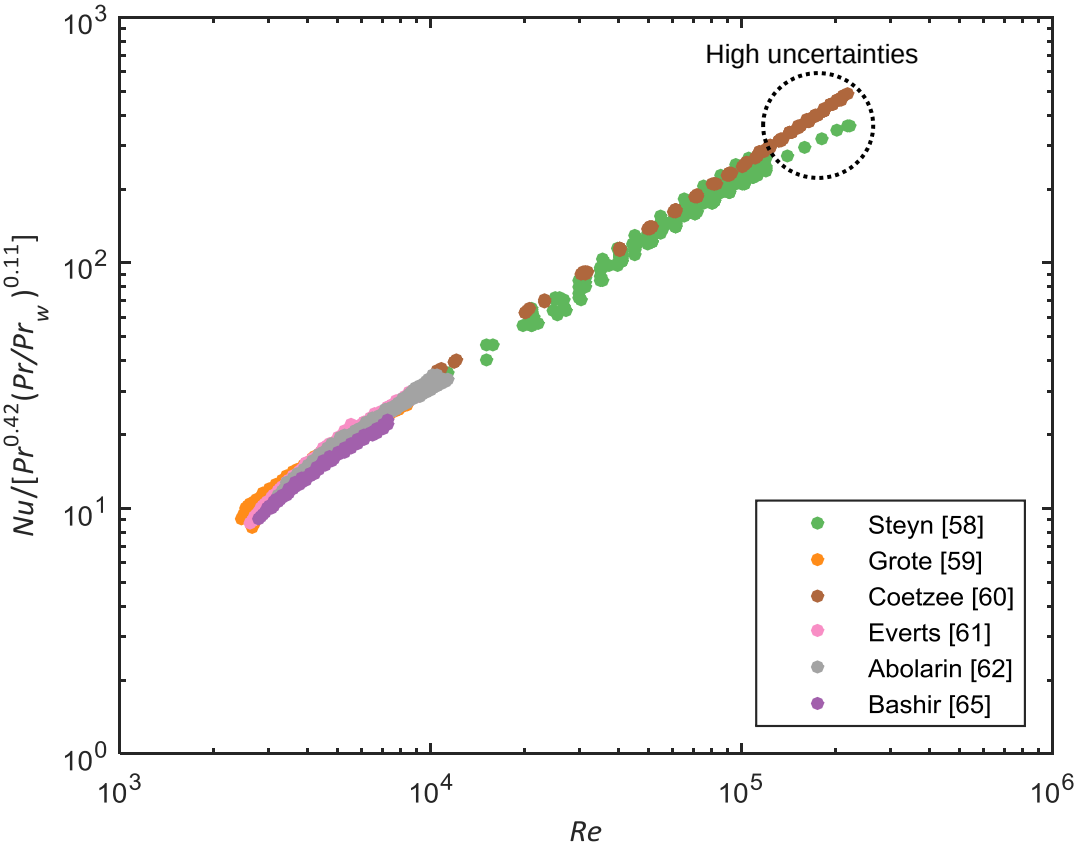

Fig. 10: Comparison of the experimental heat transfer data of this study in terms of $Nu/[Pr^{0.42}(Pr/Pr_w)^{0.11}]$ as a function of Reynolds number.

The relationship between heat transfer and pressure drop in Fig. 6 makes it possible to calculate the Nusselt numbers as a function of friction factor (Eq. (27)). To incorporate this relationship, the heat transfer results in Fig. 10 were divided by Blasius friction factor (Eq. (22)). The correlation of Blasius [90] was used, because friction factor data might not necessarily be available and it was concluded from Table 7 that this correlation is both simple and accurate. Furthermore, Gnielinski [31] found that by plotting the heat transfer results as a function of (Re – 1 000), better correlation was obtained at lower Reynolds numbers close to the transitional flow regime. For this study, it was found that best results were obtained when the heat transfer results were plotted in terms of $Nu/[Pr^{0.42}(Pr/Pr_w)^{0.11}]f$ as a function of (Re – 500). The following turbulent Nusselt number correlation was obtained by performing a power curve fit regression through the 1 180 data points, which produced a coefficient of determination of R^2 = 0.999, as shown in Fig. 11(a):

$$\frac{Nu}{Pr^{0.42}\left(\frac{Pr}{Pr_w}\right)^{0.11}f} = 0.0575(Re - 500)^{1.071} \tag{29}$$

Which can be simplified to,

$$Nu = 0.058(Re - 500)^{1.07}Pr^{0.42}\left(\frac{Pr}{Pr_w}\right)^{0.11}f \tag{30}$$

By substituting the friction factor with the Blasius correlation (Eq. (22)), the following Nusselt number for quasi-turbulent and turbulent flow was obtained:

$$Nu = 0.018Re^{-0.25}(Re - 500)^{1.07}Pr^{0.42}\left(\frac{Pr}{Pr_w}\right)^{0.11} \tag{31}$$

Fig. 11(b) indicates that Eq. (31) performed very well and was able to predict 95% of our own experimental data within 10% and the average deviation was only 4.4% (which is in the same range as our Nusselt number uncertainties of approximately 5%).

As discussed previously, Eqs. (27) and (30) will most probably not only be valid for smooth tubes, but also for rough tubes if the friction factors of the rough tube can be determined. It should be noted that with rough tubes, we refer to tubes with significant relative roughness values (ε/D) and not to tubes with enhanced surfaces. The measured relative roughness of the tubes used in our own experiments varied between 1.89×10^{-5} and 3.45×10^{-5}. These tubes could conservatively be considered as smooth tubes as the Moody chart [40] indicates that the relative roughness should increase by two orders of magnitude to 0.002, before the friction factor will increase by 5% at a Reynolds number of 10 000.

The Prandtl numbers of the experimental data of this study was limited to 3-10. Therefore, experimental data from literature [3, 16, 17, 20, 23, 29, 39, 84-89], with a Reynolds number range of 3 000-401 600 and a wider Prandtl number range of 0.47-276, were used to evaluate the performance of Eq. (31) when high Prandtl number fluids, or fluids with a Prandtl number of less than 1, are used. Fig. 12(a) compares the heat transfer data of this study and literature [3, 16, 17, 20, 23, 29, 39, 84-89]

in terms of $Nu/[Pr^{0.42}(Pr/Pr_w)^{0.11}]f$ as a function of $(Re - 500)$, while Fig. 12(b) compares the deviation between Eq. (31) and the experimental data in literature.

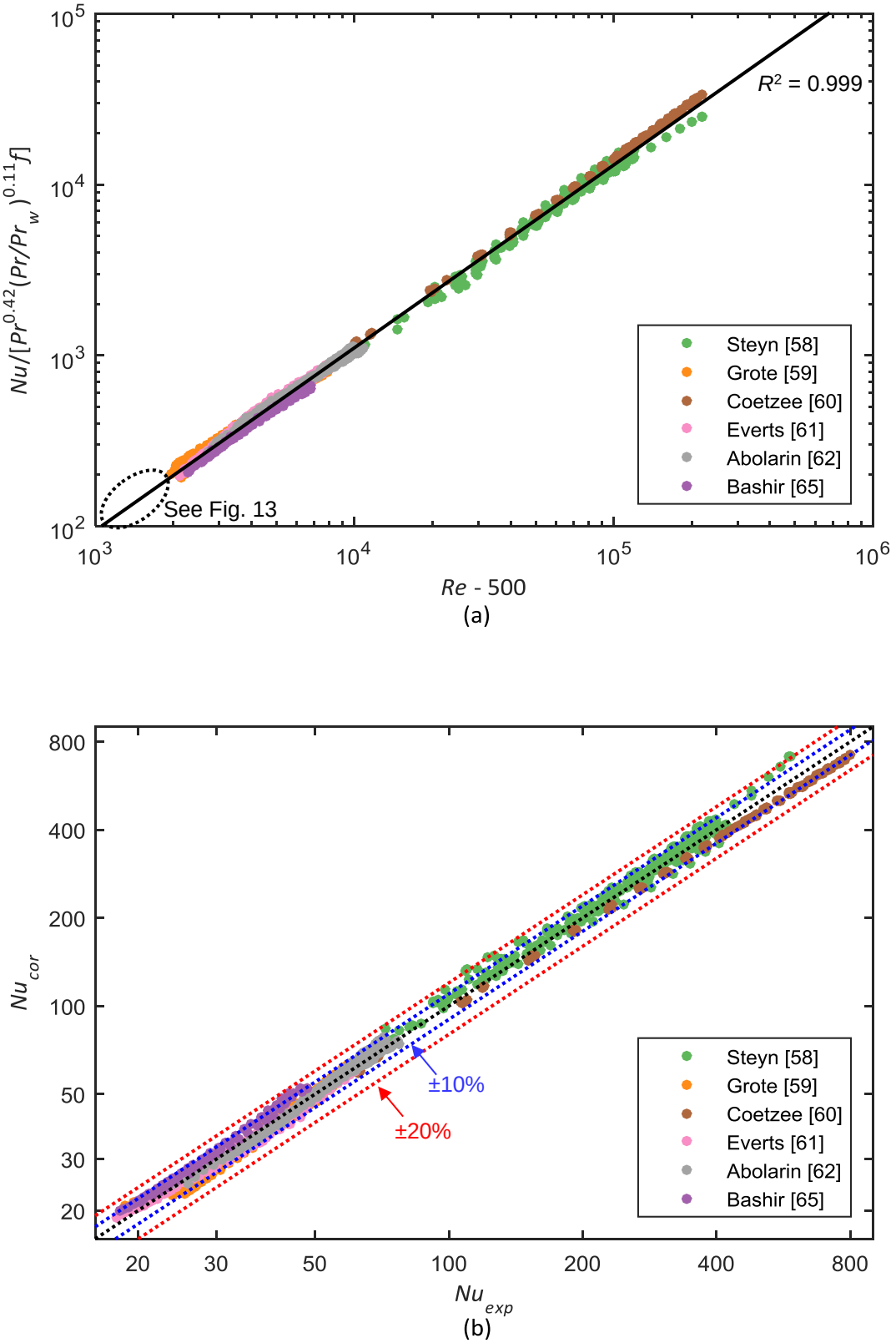

Fig. 11: Comparison of (a) the experimental heat transfer data of this study in terms of $Nu/[Pr^{0.42}(Pr/Pr_w)^{0.11}]f$ as a function of Re – 500 and (b) deviation between Eq. (31) and the experimental data of this study.

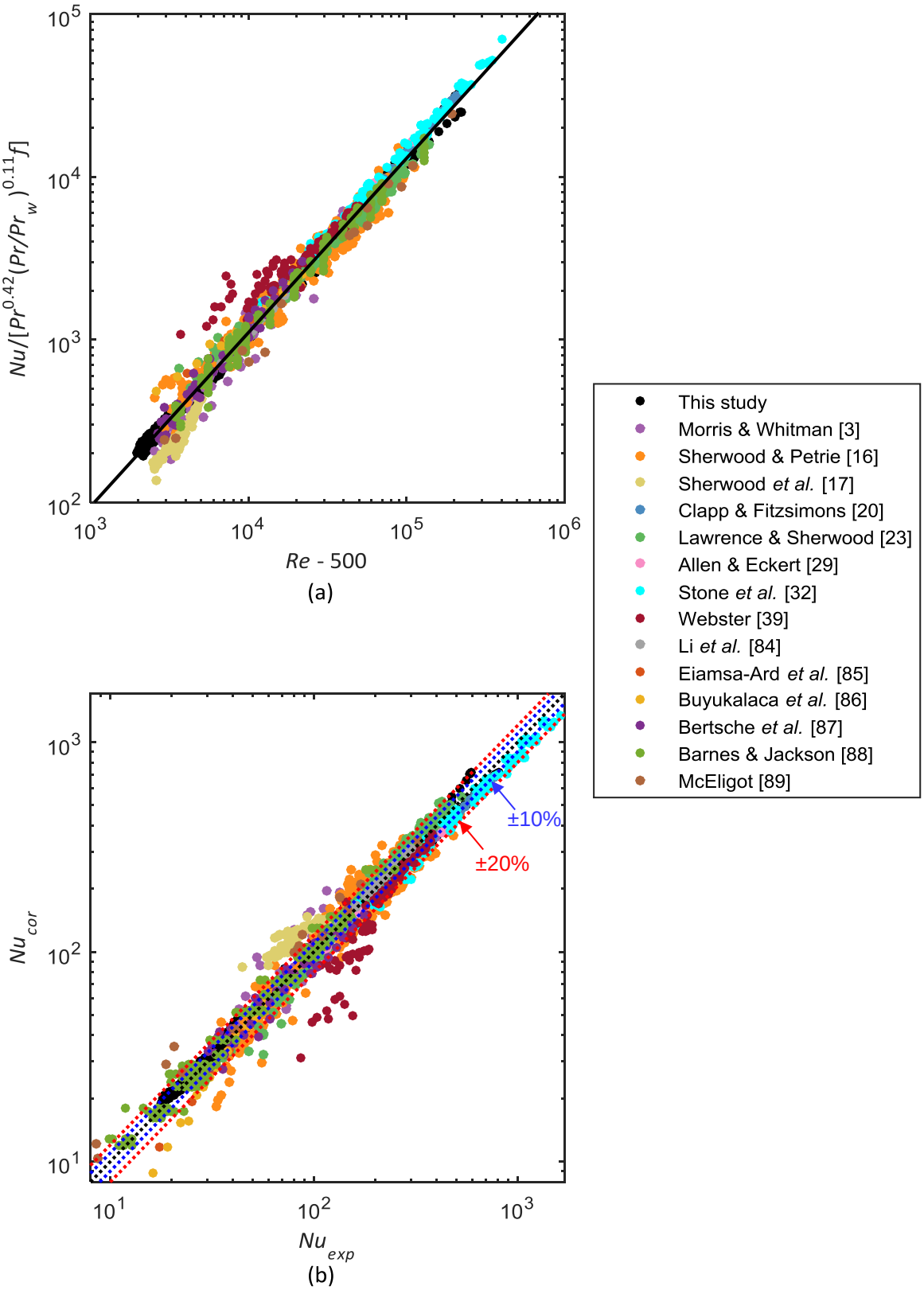

Fig. 12: Comparison of (a) the experimental heat transfer data of this study and literature [3, 16, 17, 20, 23, 29, 32, 39, 84-89] in terms of $Nu/[Pr^{0.42}(Pr/Pr_w)^{0.11}]f$ as a function of Re – 500 and (b) deviation between Eq. (31) and the experimental data in literature [3, 16, 17, 20, 23, 29, 39, 84-89].

Eq. (31) was able to predict 50% of the data within errors of 10% and 77% of the data within 20% errors and the average deviation was 15%. It should be noted that Eq. (31) was able to predict the 216 experimental data points obtained using gases [85, 86, 88, 89] with an average deviation of only 11%. Furthermore, Eq. (31) predicted the 87 high Prandtl number experimental data points of Morris and Whitman [3] and Li *et al*. [84] with an average deviation of 9%. It can therefore be concluded that Eq. (31) is a suitable correlation to use for gases (Prandtl numbers less than 1), water (low Prandtl numbers), as well as oils (high Prandtl numbers between 20 and 276). Because Eq. (31) also predicted the experimental data of Stone *et al*. [32] with a Reynolds number range of 12 000-401 600 with an average deviation of 13%, it was concluded that this correlation is suitable for very high Reynolds numbers.

The Nusselt numbers predicted using Eq. (31) were also compared with the Nusselt numbers predicted with the existing correlations in literature (Table 1) using the experimental data of this study and literature [3, 16, 17, 20, 23, 29, 39, 84-89] and the results are summarised in Table 9. This table indicates that when the experimental data of this study (relatively low Prandtl numbers) were used to compare the correlations, the correlations of Colburn [9], Petukhov [26], and Gnielinski [31] produced similar Nusselt numbers than Eq. (31). However, when the experimental data in literature (Prandtl numbers less than unity, as well as very high Prandtl numbers) were used, the correlations of Dittus and Boelter [2], Hausen [1], and Petukhov [26] produced similar Nusselt numbers than Eq. (31).

Table 9: Comparison of existing Nusselt number correlations compared with Eq. (31) using the experimental data of this study and literature [3, 16, 17, 20, 23, 29, 32, 39, 84-89].

	Eq.	Error					
		This study			Literature [3, 16, 17, 20, 23, 29, 32, 39, 84-89]		
		±10% [%]	±20% [%]	Ave [%]	±10% [%]	±20% [%]	Ave [%]
Dittus and Boelter [2]	(2)	33	80	14	75	96	6.8
Colburn [9]	(3)	86	100	6.0	37	75	14
Sieder and Tate [19]	(4)	29	66	16	91	76	13
Hausen [1]	(5)	42	93	12	44	100	4.3
Petukhov [26]	(6)	60	98	7.3	69	93	8.1
Gnielinski [31]	(7)	67	100	6.9	27	88	13

It can therefore be concluded that the agreement of the different correlations with each other is, as expected, influenced by the Prandtl number and Reynolds number. To investigate this further, Eq. (31) was compared with the existing correlations in literature (Table 1) between Reynolds numbers of 2 000 and 10^6 for Prandtl numbers of 0.7, 7 and 70. In general, it was found that between Reynolds numbers of 10 000 and 47 000, the correlations were within 20% of each other for all Prandtl numbers. However, as the Reynolds number was decreased below 10 000 (to the quasi-turbulent flow regime), or increased above 47 000, the deviation increased up to 60%. In the quasi-turbulent flow regime, the correlation of Gnielinski [31] was in good agreement with Eq. (31), while the correlation of Dittus and Boelter [2] correlated better with Eq. (31) at very high Reynolds numbers.

Because the heat transfer coefficients of developing flow are higher than for fully developed flow, Gnielinski [31] used the term $[1 + (D/L)^{2/3}]$ to account for very short tubes. From the experimental data of this study, it was found that the same term $[1 + (D/L)^{2/3}]$ can be added to Eq. (31). Therefore, the following general correlation was obtained to calculate the Nusselt numbers of quasi-turbulent and turbulent flow in short tubes:

$$Nu = 0.018Re^{-0.25}(Re - 500)^{1.07}Pr^{0.42}\left(\frac{Pr}{Pr_w}\right)^{0.11}\left[1 + \left(\frac{D}{L}\right)^{2/3}\right] \quad (32)$$

It was found that for the experimental data of this study, Eq. (32) performed slightly better than Eq. (31) and was able to predict 95% of our own experimental data within 10% and the average deviation was only 4.4%. Furthermore, Eq. (32) was able to predict 50% of the experimental data from literature [3, 16, 17, 20, 23, 29, 39, 84-89] within errors of 10% and 76% of the data within 20% errors. The average deviation was 15%.

8.3.2 Transitional flow

Although the results in Fig. 11(a) collapsed onto a single line and yielded a correlation with a coefficient of determination, R^2, of 0.999, this was only true for the quasi-turbulent and turbulent flow regimes. Once the heat transfer results in the transitional flow regime were added, as shown in Fig. 13, it became clear that other parameters need to be included to account for the heat transfer characteristics in the transitional flow regime ($Re < 3\,000$).

Everts and Meyer [43, 49] investigated the heat transfer characteristics of transitional flow and found that it was dependent on developing flow (tube length or axial position), free convection effects (Grashof number), and the type of fluid (Prandtl number). Previous work by Ghajar and Tam [69] also found that the heat transfer coefficients in the transitional flow regime were significantly affected by the inlet geometry. Taler [47] gives a comprehensive overview of the available correlations in the transitional flow regime. Although several correlations exist in literature, these correlations were either limited to specific fluids, or did not account for free convection effects. The lack of experimental data in the transitional flow regime, is probably one of the main reasons for the limited understanding and correlations that are available [44]. To develop a correlation for transitional flow, the experimental data obtained using a square-edged inlet [61, 62, 65] were used for this study. As these experiments were conducted using water, the Prandtl number range was 4-6.6. Therefore, to extend the Prandtl number range, the square-edged inlet transitional flow data of Strickland [94], obtained using ethylene glycol-water mixtures ($21.9 < Pr < 49$), were also used. It should be noted that the experimental data of this study [61, 62, 65] were average values across the tube length, while the data of Strickland [94] was obtained at a single measuring station in the fully developed region of the test section. Because fully developed flow conditions existed in the experimental data of this study [61, 62, 65], it was considered appropriate to incorporate the fully developed experimental data of Strickland [94] as well.

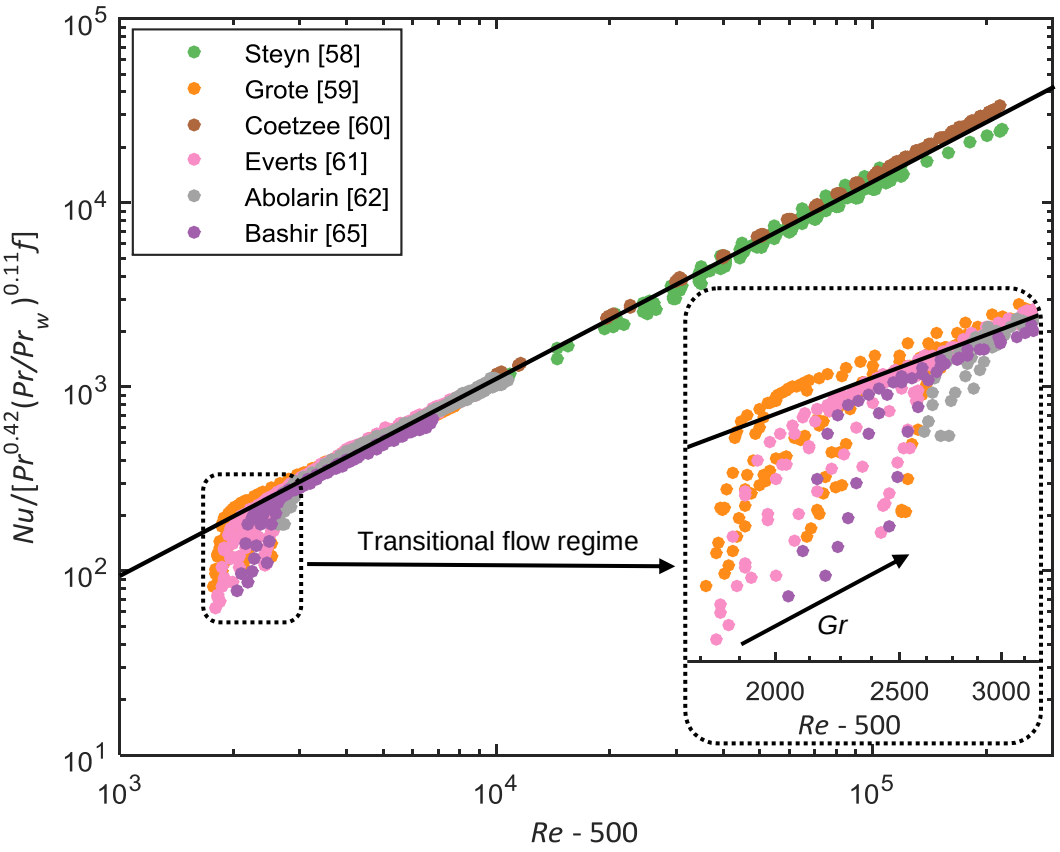

Fig. 13: Comparison of the experimental heat transfer data of this study in the transitional, quasi-turbulent and turbulent flow regimes in terms of $Nu/[Pr^{0.42}(Pr/Pr_w)^{0.11}]f$ as a function of $Re - 500$.

The Nusselt numbers were divided by $Pr^{0.33}$ and $Gr^{-0.08}$, to account for different Prandtl number fluids as well as free convection effects, and plotted as a function of Reynolds number in Fig. 14(a). Although the exponent of the Prandtl number in the turbulent correlations was 0.42, it was found that better results were obtained in the transitional flow regime when an exponent of 0.33 was used. Furthermore, the Grashof number exponent of -0.08 might seem negligible; however, the Grashof numbers ranged between 1.19×10^3 and 1.75×10^5, therefore $Gr^{-0.08}$ ranged between 0.38 and 0.60, which is significant. It was not possible to exclude the Grashof number from the transitional flow correlation, because free convection effects significantly affects the heat transfer characteristics in this flow regime [43]. A linear curve fit was performed through the 119 data points in Fig. 14(a) to obtain the following correlation that can be used to calculate the heat transfer coefficients in the transitional flow regime with a square-edged inlet:

$$Nu = (0.017Re - 30.3)Pr^{0.33}Gr^{-0.08} \tag{33}$$

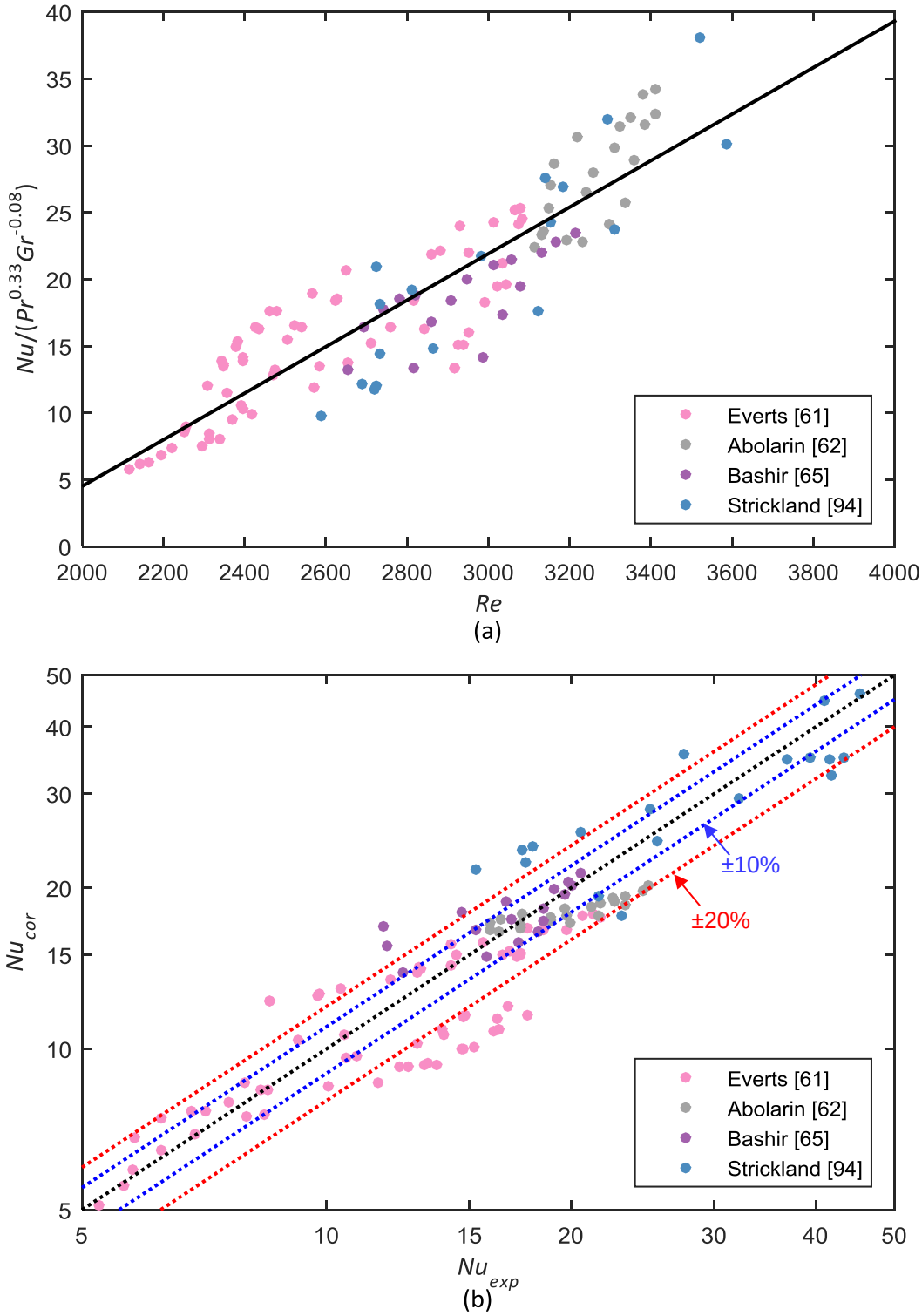

Fig. 14: Comparison of (a) the transitional experimental heat transfer data of this study and of Strickland [94], obtained using a square-edged inlet, in terms of $Nu/(Pr^{0.33}Gr^{0.08})$ as a function of Reynolds number and (b) deviation between Eq. (31) and the experimental data of this study and of Strickland [94].

The results in Fig. 14(b) indicate that Eq. (33) was able to predict 43% of the data within 10% errors and 70% of the data within 20% errors and the average deviation was 15%. It should be noted that these errors are significantly larger than for Eq. (31), which is valid for quasi-turbulent and turbulent flow regime. This is as expected, because the uncertainties of the heat transfer coefficients in the transitional flow regime are much larger (usually between 10% and 20%) than in the other flow regimes owing to the temperature and mass flow rate fluctuations that occur in this flow regime [43]. Furthermore, due to the limited transitional flow experimental data that are readily available in literature, significantly less data points were used to develop Eq. (33) than Eq. (31). The transitional flow experimental data that are available in literature were mainly for mixed convection conditions. Limited experiments were conducted for forced convection conditions; however, the uncertainties are relatively high [43, 57, 63]. Furthermore, the available data were for a constant heat flux boundary condition only and not for a constant surface temperature boundary condition. Although the boundary condition has a negligible influence in the turbulent flow regime, the laminar Nusselt numbers were affected (Nu = 4.36 for a constant heat flux boundary condition and Nu = 3.66 for a constant surface temperature boundary condition). Furthermore, the influence of free convection effects were stronger with a constant heat flux boundary condition than with a constant surface temperature boundary condition [70]. It can therefore be expected that the boundary condition will also affect the heat transfer characteristics in the transitional flow regime, especially when the mixed convection conditions exist.

8.3.3 Single correlation for laminar, transitional, quasi-turbulent and turbulent flow

Meyer and Everts [57] developed the following correlation to calculate the average laminar Nusselt numbers for developing and fully developed flow in both forced and mixed convection conditions:

$$Nu = 4.36 + Nu_1 + Nu_2 \tag{34}$$

$$Nu_1 = \frac{1}{L}\left(-0.84\, Pr^{-0.2} Lt_{MCD} + 0.72(ReD)^{0.54} Pr^{0.34} Lt_{MCD}^{0.46}\right)$$

$$Nu_2 = \frac{1}{L}((0.207 Gr^{0.305} - 1.19) Pr^{0.42} (ReD)^{-0.08} (L - Lt_{MCD})$$

$$Lt_{MCD} = \frac{2.4 RePr^{0.6} D}{Gr^{0.57}} \text{ for } L > Lt_{MCD}$$

$$Lt_{MCD} = L \text{ for } L < Lt_{MCD}$$

By making use of the method of Churchill and Usagi [95], a single correlation that is valid for all flow regimes was obtained:

$$Nu = \left[Nu_{Eq.(34)}^{10} + \left(Nu_{Eq.(33)}^{-8} + Nu_{Eq.(31)}^{-8}\right)^{-10/8}\right]^{0.1} \tag{35}$$

Eq. (34) (laminar flow), Eq. (33) (transitional flow) and Eq. (31) (quasi-turbulent and turbulent flow) should be used to calculate $Nu_{Eq.(34)}$, $Nu_{Eq.(33)}$ and $Nu_{Eq.(31)}$, respectively. The exponents of -8 and 10 that were used in Eq. (35) may appear to be high (as exponents of 3 and 4 are usually used). However, these high exponents were chosen to ensure that the error at the intersection of Eqs. (34) and (31) (at the start of the transitional flow regime) and Eqs. (31) and (33) (at the end of the transitional flow regime) was always less than 10%, irrespective of the Reynolds number, Prandtl number and Grashof number. It should be noted that although Eqs. (31) and (34) are valid for low and high Prandtl number fluids, different inlet geometries and test sections with a wide range of diameters and lengths, Eq. (33) was developed using data with a Prandtl number range of 4-49 and a square-edged inlet only. The performance of Eq. (35) was evaluated using 837 data points with a Reynolds number range of 597-46 001, Prandtl number range of 3-140 and Grashof number range of 334-4×10^5. It was found that Eq. (35) was able to predict 60% of the data within errors of 10% and 79% of the data within 20% errors. The average deviation was 18%.

Gnielinski [44] proposed a different, but simpler, method to obtain a correlation that links the laminar and turbulent Nusselt number correlations:

$$Nu = (1-\gamma)Nu_{lam,2300} + \gamma Nu_{turb,4000} \tag{36}$$

$$\gamma = \frac{Re - 2\,300}{4\,000 - 2\,300}$$

Therefore, separate correlations for laminar and turbulent flow were presented and the Nusselt number at a Reynolds number of 2 300 was calculated using the laminar correlation, while the turbulent correlation was used to calculate the Nusselt number at a Reynolds number of 4 000. Eq. (36) was then used to calculate the Nusselt numbers in the transitional flow regime by means of interpolation.

Although this method is simple and easy to implement, the following should be kept in mind when using this method: (1) The laminar correlation that was provided are suited for forced convection conditions and did not account for free convection effects. The Nusselt number at the start of transition will thus be underpredicted if mixed convection conditions exist [57]. (2) The Reynolds number at which transition starts is not necessarily 2 300, but will depend on the inlet geometry, tube diameter, developing flow, Prandtl number, as well as free convection effects [43]. (3) The Reynolds number at which transition ends is also affected by free convection effects, developing flow and fluid properties [43]. (4) The gradient of the Nusselt number in the transitional flow regime is significantly affected by free convection effects and developing flow [43, 49, 57]. Therefore, Eq. (36) might be a simple correlation to use to get an indication of the Nusselt numbers in the transitional flow regime, but Eq. (35) will give a better representation of the actual transitional Nusselt numbers.

Furthermore, it should be noted that the following correlation can be extracted from Eq. (35) to obtain a single correlation that is valid for transitional to turbulent flow:

$$Nu = \left(Nu_{Eq.(33)}^{-8} + Nu_{Eq.(31)}^{-8}\right)^{-1/8} \quad (37)$$

where Eq. (33) for transitional flow, and Eq. (31) for quasi-turbulent and turbulent flow can be used to calculate $Nu_{\text{Eq.(33)}}$ and $Nu_{\text{Eq.(31)}}$, respectively. Because Eq. (33) was developed using data for a constant heat flux boundary condition and a square-edged inlet only, Eq. (37) may be accurate for fluids with Prandtl numbers between 4 and 49 but will become less accurate as the Prandtl number is increased. For fluids with Prandtl numbers between 4 and 49, it was found that Eq. (37) was able to predict 64% of the data within errors of 10% and 90% of the data within 20% errors. The average deviation was 9%.

8.3.4 Summary of correlations

Table 10 gives a summary of the correlations and their ranges that were presented in this paper. The laminar correlation (Eq. (34)) was developed by Meyer and Everts [57]. This correlation is valid for developing and fully developed laminar flow in both forced and mixed convection conditions and was therefore selected to be used in the laminar flow part of Eq. (35). For continuity from laminar to turbulent flow, Eq. (33) was developed to be used in the transitional flow part of Eq. (35).

Because this study focussed on quasi-turbulent and turbulent flow, three sets of correlations are presented. Eqs. (27) and (28) are easy to use and quite accurate, while Eqs. (30) and (31) are more accurate. Eq. (32) is specifically for short tubes, but can of course be used for short and long tubes. Furthermore, Eqs. (27) and (30) are a function of friction factor, while the Blasius friction factor for smooth tubes has been incorporated in Eqs. (28) and (31). Therefore, Eqs. (28) and (31) are valid for smooth tubes only, but it can be postulated that Eqs. (27) and (30) may be suitable for rough tubes if the appropriate friction factors are used. As Eq. (31) is the most accurate correlation for quasi-turbulent and turbulent flow, it is suggested that this correlation is used in the turbulent flow part of Eq. (35). If no experimental data in the laminar flow regime are available and only data in the transitional, quasi-turbulent and turbulent flow regimes are available, Eq. (37) can be used to calculate the Nusselt numbers of transitional to turbulent flow.

Table 10: Summary of the correlations presented in this study

	Eq.	Range	Data points	±10% [%]	±20% [%]	Ave [%]
Laminar [57] $Nu = 4.36 + Nu_1 + Nu_2$ $Nu_1 = \frac{1}{L}(-0.84\,Pr^{-0.2}Lt_{MCD} + 0.72(ReD)^{0.54}Pr^{0.34}Lt_{MCD}^{0.46})$ $Nu_2 = \frac{1}{L}((0.207Gr^{0.305} - 1.19)Pr^{0.42}(ReD)^{-0.08}(L - Lt_{MCD})$ $Lt_{MCD} = \frac{2.4RePr^{0.6}D}{Gr^{0.57}}$ for $L > Lt_{MCD}$ $Lt_{MCD} = L$ for $L < Lt_{MCD}$	(34)	$48 \leq Re \leq 3\,217$, $2.9 \leq Pr \leq 282$, $2.6 \leq Gz \leq 1.14\times10^5$, $5.5 \leq Gr \leq 4.51\times10^5$	495*	98	100	3.6
Transitional $Nu = (0.017Re - 30.3)Pr^{0.33}Gr^{-0.08}$	(33)	$2\,115 \leq Re \leq 3\,586$, $4 \leq Pr \leq 49$, $1.19\times10^3 \leq Gr \leq 1.75\times10^5$	119 101**	43 46	70 73	15 14
Quasi-turbulent and turbulent (Simple) $Nu = 0.041Re^{1.117}Pr^{1/3}f$ ***	(27)	$2\,445 < Re < 401\,600$ $0.5 < Pr < 276$	2 351	57	80	12
$Nu = 0.013Re^{0.867}Pr^{1/3}$	(28)	$0.85 < (Pr/Pr_w)^{0.11} < 1.17$	1 180**	79	96	6.4
Quasi-turbulent and turbulent (Lengthy, but more accurate) $Nu = 0.058(Re - 500)^{1.07}Pr^{0.42}\left(\frac{Pr}{Pr_w}\right)^{0.11}f$ ***	(30)	$2\,445 < Re < 401\,600$ $0.5 < Pr < 276$ $0.85 < (Pr/Pr_w)^{0.11} < 1.17$	2 351	72	88	9.5
$Nu = 0.018Re^{-0.25}(Re - 500)^{1.07}Pr^{0.42}\left(\frac{Pr}{Pr_w}\right)^{0.11}$	(31)		1 180**	95	100	4.4
Quasi-turbulent and turbulent (Short tubes) $Nu = 0.018Re^{-0.25}(Re - 500)^{1.07}Pr^{0.42}\left(\frac{Pr}{Pr_w}\right)^{0.11}\left[1 + \left(\frac{D}{L}\right)^{2/3}\right]$	(32)	$2\,445 < Re < 401\,600$ $0.5 < Pr < 276$ $1.0081 < [1 + (D/L)^{2/3}] < 1.15$ $0.85 < (Pr/Pr_w)^{0.11} < 1.17$	2 351 1 180**	73 95	88 100	9.8 4.4
Transitional, quasi-turbulent and turbulent $Nu = \left(Nu_{Eq.(33)}^{-8} + Nu_{Eq.(31)}^{-8}\right)^{-1/8}$	(37)	$2\,282 \leq Re \leq 46\,001$, $4 \leq Pr \leq 49$, $334 \leq Gr \leq 1.75\times10^5$ $1.0 < (Pr/Pr_w)^{0.11} < 1.02$	584 542**	64 63	90 89	9.3 9.5
All flow regimes $Nu = \left[Nu_{Eq.(34)}^{10} + \left(Nu_{Eq.(33)}^{-8} + Nu_{Eq.(31)}^{-8}\right)^{-10/8}\right]^{0.1}$	(35)	$597 \leq Re \leq 46\,001$, $3 \leq Pr \leq 139$, $334 \leq Gr \leq 4.04\times10^5$	837 768**	60 60	79 79	18 18

Notes: *Meyer and Everts [57]; **Performance evaluated using the experimental data of this study; ***Suitable for rough tubes when appropriate friction factor is used

9. CONCLUSIONS

In the past century, several correlations to determine the heat transfer coefficients in smooth tubes in the turbulent flow regime were developed. Unfortunately, when these equations were developed, no uncertainty analyses were conducted. The purpose of this study was to conduct heat transfer and pressure drop experiments in the quasi-turbulent and turbulent flow regimes and to develop an accurate heat transfer correlation, that can be combined with recently developed laminar and transitional flow correlations, to obtain a single correlation that is valid for all flow regimes. The main objectives were: (1) To take accurate heat transfer and pressure drop measurements on a smooth horizontal tube in the quasi-turbulent and turbulent flow regimes and to quantify the uncertainties of the Reynolds numbers, Nusselt numbers and friction factors. (2) To evaluate and compare the existing turbulent correlations in literature with this data. (3) To develop a new correlation from this data and to compare it to the existing correlations and experimental data in literature. (4) To link this work in the quasi-turbulent and turbulent flow regimes to recent work conducted in the laminar and transitional flow regimes by providing a single Nusselt number correlation that is valid for all flow regimes. Heat transfer and pressure drop measurements were taken using two different test section configurations. The first configuration consisted of a tube-in-tube heat exchanger to obtain a constant surface temperature boundary conditions, for both heating and cooling conditions. The second test section configuration consisted of single tubes being electrically heated at a constant heat flux. Different test sections covering a range of tube diameters from 4 mm to 19 mm and a range of tube lengths from 1 m to 9.5 m, were used. A total of 1 180 experimental data points were collected from careful experiments that were conducted between Reynolds numbers of 2 445 and 220 800.

The surface temperatures were obtained by either direct temperature measurements or by making use of the Wilson plot method. It was found that both methods yielded accurate heat transfer coefficients and confirmed that the turbulent heat transfer coefficients were independent of the boundary condition. An uncertainty analysis was conducted to quantify the uncertainties of the experimental data of this study. The Reynolds number, Nusselt number and friction factor uncertainties were approximately 2%, 5% and 10% respectively.

By making use of the relationship between heat transfer and pressure drop and accounting for different Prandtl number fluids, variable fluid properties with temperature, as well as different test section dimensions and configurations, heating methods and boundary conditions, three versatile Nusselt number correlations for flow in the quasi-turbulent and turbulent flow regimes, were obtained: (1) a simple, yet accurate, correlation, (2) a more accurate correlation and (3) a correlation specifically for short tubes. All three correlations performed very well. The more accurate correlation was able to predict 95% of the data within 10% and the average deviation was only 4.4%. Furthermore, it was able to predict a wide range of experimental data in literature (with unknown uncertainties) with a Prandtl number range of 0.47-276 and Reynolds number range of 3 000-401 600 with an average deviation was

15%. It can therefore be concluded that this correlation is able to accurately predict the Nusselt numbers in the quasi-turbulent and turbulent flow regimes. For continuity from laminar to turbulent flow, a correlation to predict the heat transfer coefficients in the transitional flow regime was also developed using the experimental data of this study. This correlation was able to predict 41% of the data within 10%, 80% of the data within 20%, and the average deviation was 13%. Finally, a single Nusselt number correlation that is valid for laminar, transitional, quasi-turbulent and turbulent flow was also presented.

10. ACKNOWLEDGEMENTS

The funding obtained from both the DST and NRF from South Africa are duly appreciated. We would also like to acknowledge the assistance and recommendations of Professor Volker Gnielinski (Karlsruher Institut für Technologie) during a visit to our laboratory in 2010, as well as his feedback as external examiner of Coetzee [60] and his subsequent email correspondence. Coetzee, Grote and Steyn were master's degree students and Everts a PhD student/postdoctoral fellow. All studied under the supervision of the first author.

REFERENCES

[1] H. Hausen, Heat transfer in counterflow, parallel-flow, and cross-flow, McGraw-Hill, New York, 1983.
[2] F. Dittus, L.M.K. Boelter, Heat Transfer in Automobile Radiators of the Tubular Type, University of California Publications in Engineering, 2(12) (1930) 443-461.
[3] F.H. Morris, W.G. Whitman, Heat transfer for oils and water in pipes, Industrial and Engineering Chemistry, 20(3) (1928) 234-240.
[4] W. Nusselt, Der wärmeübergang on rohrleitungen, Zeitschrift des Vereines Deutscher Ingenieure, Heft 191-192 (1910) 1750-1755.
[5] E. Josse, Versuche über oberklächenkondensation, insbesondere für dampfturbinen, Zeitschrift des Vereines Deutscher Ingenieure, 53 (1909) 322-330.
[6] W.H. McAdams, T.H. Frost, Heat transfer for water flowing inside pipes, Refrigerating Engineering, 10(9) (1924) 323-334.
[7] B. Hilliger, Untersuchungen über die wirkung von einlagekörpen in den rauchröhren von lokomiikesselu, Zeitschr. des Vereines deutscher Ingenieure, 60 (1916) 889.
[8] E. Schulze, Versuche zur bestimmung der wärmeübergangszahl von luft und rauchgas in technischen rohren, Wärmestelle des Vereines deutscher Eisenhüttenleute, (117) (1928).
[9] A.P. Colburn, A method of correlating forced convection heat transfer data and a comparison with fluid friction, Transactions of American Institute of Chemical Engineers, 29 (1933) 174-210.
[10] R. Poensgen, Ueber die wämeübertragung von strömendem überhitztem wasserdampf an rohrwandungen und von heizgasen as wasserdampf, Zeitschrift des Vereines Deutscher Ingenieure, 60 (1916) 27-32.
[11] W.H. McAdams, T.H. Frost, Heat transfer by conduction and convection II- Liquids flowing through pipes, Journal of Industrial & Engineering Chemistry, 14(12) (1922) 1101-1104.
[12] C.S. Keevil, W.H. McAdams, How heat transmission affects fluid friction in pipes, Chemical and Mettallurgical Engineering, 36(8) (1929) 464-467.
[13] A.P. Colburn, O.A. Hougen, III-Flow of fluids at low velocities, Industrial and Engineering Chemistry, 22(5) (1930) 534-539.
[14] A. Eagle, R.M. Ferguson, On the coefficient of heat transfer from the internal surface of tube walls, Proceedings of the Royal Society. Series A, Containing Papers of a Mathematical and Physical Character, (1930) 540-566.

[15] R. Hermann, T.H. Burbach, Strömungswiderstand und wärmeübergang in rohren, 1930.
[16] T.K. Sherwood, J.M. Petrie, Heat transmission to liquids flowing in pipes, Industrial and Engineering Chemistry, 24(7) (1932) 736-745.
[17] T.K. Sherwood, D.D. Kiley, G.E. Mangsen, Heat transmission to oil flowing in pipes effect of tube length, Industrial & Engineering Chemistry, 24(3) (1932) 273-277.
[18] H. Kraussold, Gebiete Ingenieurw. 2, in: Forschungsheft 351, 1931.
[19] E.N. Sieder, G.E. Tate, Heat transfer and pressure drop of liquids in tubes, Industrial Engineering Chemistry, 28 (1936) 1429-1435.
[20] M.H. Clapp, O. FitzSimons, The effect of heat transfer on friction factors in Fanning's equation, Masters dissertation, Massachusetts Intitute of Technology, Massachusetts, 1929.
[21] C.G. Kirkbride, W.L. McCabe, Heat transfer to liquids in viscous flow, Industrial and Engineering Chemistry, 23(6) (1931) 625-631.
[22] T.B. Drew, J.J. Hogan, W.H. McAdams, Heat transfer in stream-line flow, Industrial and Engineering Chemistry, 23(8) (1931) 936-945.
[23] A.E. Lawrence, T.K. Sherwood, Heat transmission to water flowing in pipes, Industrial and Engineering Chemistry, 23(3) (1931) 301-309.
[24] T.B. Drew, Heat transfer in stream-line flow II. Experiments with glycerol, Industrial and Engineering Chemistry, 24(2) (1932) 152-157.
[25] C.S. Keevil, PhD Thesis, Massaschusettes Institute of Technology, Cambridge, 1930.
[26] B.S. Petukhov, Heat transfer and friction in turbulent pipe flow with variable physical properties, in: J.P. Hartnett, I. T.F. (Eds.) Advances in Heat Transfer, Academic Press, New York, 1970, pp. 503-564.
[27] V.V. Yakovlev, Local and mean heat-transfer for a turbulent flow o nonboiling water in a tube with high heat loads, Soviet Journal of Atomic Energy, 8(3) (1960) 221-224.
[28] B.S. Petukhov, L.I. Roizen, Teplofiz. Vysok. Temperatur, 1(3) (1963) 416-424.
[29] R. Allen, E. Eckert, Friction and heat-transfer measurements to turbulent pipe flow of water (Pr = 7 and 8) at uniform wall heat flux, Journal of Heat Transfer, 86(3) (1964) 301-310.
[30] L.S. Sterman, V.V. Petukjov, Investigation of the heat transfer to organic liquids, in: A.V. Lykov, B.M. Smol'skii (Eds.) Heat and Mass Transfer, 1965.
[31] V. Gnielinski, New equations for heat and mass-transfer in turbulent pipe and channel flow, International Chemical Engineering, 16(2) (1976) 359-368.
[32] J.P. Stone, C.T. Ewing, R.R. Miller, Heat-transfer studies on some stable organic fluids in a forced convection loop, Journal of Chemical & Engineering Data, 7(4) (1962) 519-525.
[33] W. Hufschmidt, E. Burck, W. Riebold, Die bestimmung örtlicher und mittlerer wärmeübergangszahlen in rohren bei hohen wärmestromdichten, Int. J. Heat Mass Transf., 9(6) (1966) 539-565.
[34] W. Hufschmidt, E. Burck, Der einfluss temperaturabhängiger stoffwerte auf den wärmeübergang bei turbulenter strömung von flüssigkeiten in rohren bei hohen wärmestromdichten und prandtlzahlen, Int. J. Heat Mass Transf., 11(6) (1968) 1041-1048.
[35] M.N. Ivanovskii, Rapid method of measuring the average heat transfer coefficient in a tube, Department of Commerce, Washington, 1962.
[36] I.T.A.e. Alad'jev, N.A. Vel'tishchev, N.S. Kondrat'ev, Heat transfer by convection at high pressure, Foreign Technol. Div., Wright-Patterson AFB, Ohio.
[37] M.A.M. Mikheyev, Mean heat transfer of fluids flowing in tubes, Foreign Technol. Div., Wright-Patterson AFB, Ohio.
[38] H. Reinecke, Uber den warmeubergang von kurzen durchstromten rohren und querumstromten zylindren verschiedener anordnung an zahe flussigkeiten verschiedener Prandtl-zahl bei kleinen temperaturdifferenzen (Heat transfer for vsicous liquids of different Prandtl number flow through tubes and across cylinders of different orientation for small temperature differences), Dissertation D17, Techn. Hocshule Darmstadt 1969.
[39] G.C. Webster, Some experiments on the condensation of steam, Transactions of the Institution of Engineers and Shipbuilders in Scotland, 57 (1913) 58-105.
[40] Y.A. Cengel, A.J. Ghajar, Heat and Mass Transfer: Fundamentals and Applications, 5th ed., McGraw-Hill, 2015.

[41] H. Zhao, X. Li, X. Wu, New friction factor and Nusselt number equations for turbulent convection of liquids with variable properties in circular tubes, Int. J. Heat Mass Transf., 124 (2018) 454-462.
[42] O. Büyükalaca, J.D. Jackson, The correction to take account of variable property effects on turbulent forced convection to water in a pipe, Int. J. Heat Mass Transf., 41(4-5) (1998) 665-669.
[43] M. Everts, J.P. Meyer, Heat transfer of developing and fully developed flow in smooth horizontal tubes in the transitional flow regime, Int. J. Heat Mass Transf., 117 (2018) 1331-1351.
[44] V. Gnielinski, On heat transfer in tubes, Int. J. Heat Mass Transf., 63 (2013) 134-140.
[45] P.K. Namburu, D.K. Das, K.M. Tanguturi, R.S. Vajjha, Numerical study of turbulent flow and heat transfer characteristics of nanofluids considering variable properties, Int. J. Therm. Sci., 48(2) (2009) 290-302.
[46] J.P. Abraham, E.M. Sparrow, J.C.K. Tong, Heat transfer in all pipe flow regimes: laminar, transitional/intermittent, and turbulent, Int. J. Heat Mass Transf., 52(3-4) (2009) 557-563.
[47] D. Taler, A new heat transfer correlation for transition and turbulent fluid flow in tubes, Int. J. Therm. Sci., 108 (2016) 108-122.
[48] D.M. McEligot, X. Chu, R.S. Skifton, E. Laurien, Internal convective heat transfer to gases in the low-Reynolds-number "turbulent" range, Int. J. Heat Mass Transf., 121 (2018) 1118-1124.
[49] M. Everts, J.P. Meyer, Relationship between pressure drop and heat transfer of developing and fully developed flow in smooth horizontal circular tubes in the laminar, transitional, quasi-turbulent and turbulent flow regimes, Int. J. Heat Mass Transf., 117 (2018) 1231-1250.
[50] D. Taler, Simple power-type heat transfer correlations for turbulent pipe flow in tubes, Journal of Thermal Science, 26(4) (2017) 339-348.
[51] W. Yu-ting, L. Bin, M. Chong-fang, G. Hang, Convective heat transfer in the laminar-turbulent transition region with molten salt in a circular tube, Exp. Therm. Fluid Sci., 33(7) (2009) 1128-1132.
[52] A.R. Sajadi, M.H. Kazemi, Investigation of turbulent convective heat transfer and pressure drop of TiO 2/water nanofluid in circular tube, International Communications in Heat and Mass Transfer, 38(10) (2011) 1474-1478.
[53] M.M. Heyhat, F. Kowsary, A.M. Rashidi, S. Alem Varzane Esfehani, A. Amrollahi, Experimental investigation of turbulent flow and convective heat transfer characteristics of alumina water nanofluids in fully developed flow regime, International Communications in Heat and Mass Transfer, 39(8) (2012) 1272-1278.
[54] Y. Li, K. Fukuda, Q. Liu, M. Shibahara, Turbulent heat transfer with FC-72 in small diameter tubes, Int. J. Heat Mass Transf., 103 (2016) 428-434.
[55] F.W. Dittus, L.M.K. Boelter, Heat transfer in automobile radiators of the tubular type, International Communications in Heat and Mass Transfer, 12 (1985) 3-22.
[56] A.P. Colburn, A method of correlating forced convection heat-transfer data and a comparison with fluid friction, Int. J. Heat Mass Transf., 7(12) (1964) 1359-1384.
[57] J.P. Meyer, M. Everts, Single-phase mixed convection of developing and fully developed flow in smooth horizontal circular tubes in the laminar and transitional flow regimes, Int. J. Heat Mass Transf., 117 (2018) 1251-1273.
[58] M. Steyn, J.P. Meyer, Heat transfer coefficients for tubes in the turbulent single phase flow regime with a focus on uncertainty, in: 15th International Heat Transfer Conference (IHTC-15), Kyoto, Japan, 2014.
[59] J.P. Meyer, T.J. McKrell, K. Grote, The influence of multi-walled carbon nanotubes on single-phase heat transfer and pressure drop characteristics in the transitional flow regime of smooth tubes, Int. J. Heat Mass Transf., 58(1-2) (2013) 597-609.
[60] N. Coetzee, Heat transfer coefficients of smooth tubes in the turbulent flow regime, Masters dissertation, University of Pretoria, Pretoria, 2015.
[61] M. Everts, Single-phase mixed convection of developing and fully developed flow in smooth horizontal circular tubes in the laminar, transitional, quasi-turbulent and turbulent flow regimes, PhD thesis, University of Pretoria, Pretoria, 2017.
[62] J.P. Meyer, S.M. Abolarin, Heat transfer and pressure drop in the transitional flow regime for a smooth circular tube with twisted tape inserts and a square-edged inlet, Int. J. Heat Mass Transf., 117 (2018) 11-29.
[63] M. Everts, J.P. Meyer, Flow regime maps for smooth horizontal tubes at a constant heat flux, Int. J. Heat Mass Transf., 117 (2018) 1274-1290.

[64] J.P. Meyer, M. Everts, A.T.C. Hall, F.A. Mulock Houwer, M. Joubert, L.M.J. Pallent, E.S. Vause, Inlet tube spacing and protrusion effects on multiple circular tubes in the laminar, transitional and turbulent flow regimes, Int. J. Heat Mass Transf., 118 (2018) 257-274.
[65] A.I. Bashir, J.P. Meyer, Experimental investigation of convective heat transfer in the transitional flow regime of an inclined smooth tube, in: 16th International Heat Transfer Conference (IHTC16), Beijing, China, 2018.
[66] M. Everts, Heat transfer and pressure drop of developing flow in smooth tubes in the transitional flow regime, Master's dissertation, University of Pretoria, Pretoria, 2014.
[67] A.J. Ghajar, L.M. Tam, Laminar-transition-turbulent forced and mixed convective heat transfer correlations for pipe flows with different inlet configurations, in: Winter Annual Meeting of the American Society of Mechanical Engineers, Publ by ASME, New York, United States, 1991, pp. 15-23.
[68] A.J. Ghajar, K.F. Madon, Pressure drop measurements in the transition region for a circular tube with three different inlet configurations, Exp. Therm. Fluid Sci., 5(1) (1992) 129-135.
[69] A.J. Ghajar, L.M. Tam, Heat transfer measurements and correlations in the transition region for a circular tube with three different inlet configurations, Exp. Therm. Fluid Sci., 8(1) (1994) 79-90.
[70] A.J. Ghajar, L.M. Tam, Flow regime map for a horizontal pipe with uniform wall heat flux and three inlet configurations, Exp. Therm. Fluid Sci., 10(3) (1995) 287-297.
[71] L.M. Tam, A.J. Ghajar, Effect of inlet geometry and heating on the fully developed friction factor in the transition region of a horizontal tube, Exp. Therm. Fluid Sci., 15(1) (1997) 52-64.
[72] L.M. Tam, A.J. Ghajar, The unusual behavior of local heat transfer coefficient in a circular tube with a bell-mouth inlet, Exp. Therm. Fluid Sci., 16(3) (1998) 187-194.
[73] L.M. Tam, A.J. Ghajar, H.K. Tam, S.C. Tam, Development of a flow regime map for a horizontal pipe with the multi-classification Support Vector Machines, in: 2008 ASME Summer Heat Transfer Conference (HT2008), Jacksonville, USA, 2009, pp. 537-547.
[74] A.J. Ghajar, C.C. Tang, W.L. Cook, Experimental investigation of friction factor in the transition region for water flow in minitubes and microtubes, Heat Transfer Eng, 31(8) (2010) 646-657.
[75] H.K. Tam, L.M. Tam, A.J. Ghajar, C.W. Cheong, Development of a unified flow regime map for a horizontal pipe with the support vector machines, in: 2nd International Symposium on Computational Mechanics (ISCM II), Hong Kong, 2010, pp. 608-613.
[76] H.K. Tam, L.M. Tam, A.J. Ghajar, S.C. Tam, T. Zhang, Experimental investigation of heat transfer, friction factor, and optimal fin geometries for the internally microfin tubes in the transition and turbulent regions, J. Enhanced Heat Transf., 19(5) (2012) 457-476.
[77] H.K. Tam, L.M. Tam, A.J. Ghajar, Effect of inlet geometries and heating on the entrance and fully-developed friction factors in the laminar and transition regions of a horizontal tube, Exp. Therm. Fluid Sci., 44 (2013) 680-696.
[78] R. Rayle, Influence of orifice geometry on static pressure measurements, American Society of Mechanical Engineers, 1959.
[79] A. Bakker, R.D. LaRoche, E.M. Marshall, Laminar flow in static mixers with helical elements, in: The Online CFM Book, 2000.
[80] D.E. Briggs, E.H. Young, Modified Wilson plot techniques for obtaining heat transfer correlations for shell and tube heat exchangers, Chemical Engineering Symposium Series, 92(65) (1969) 35-45.
[81] R.K. Shah, Assessment of the modified Wilson Plot techniques for obtaining heat exchanger design data, in: 9th International Heat Transfer Conference, Jerusalem, 1990, pp. 51-56.
[82] E.E. Wilson, A basis for rational design of heat transfer apparatus, ASME Journal of Heat Transfer, 37 (1915) 47-82.
[83] P.F. Dunn, Measurement and Data Analysis for Engineering and Science, 2nd ed., CRC Press, United States of America, 2010.
[84] X.-W. Li, J.-A. Meng, Z.-X. Li, Experimental study of single-phase pressure drop and heat transfer in a micro-fin tube, Exp. Therm. Fluid Sci., 32 (2007) 641-648.
[85] S. Eiamsa-Ard, V. Kongkaitpaiboon, P. Promvonge, Thermal performance assessment of turbulent tube flow through wire coil turbulators, Heat Transfer Eng, 32(11-12) (2011) 957-967.
[86] O. Buyukalaca, V. Ozceyhan, S. Gunes, Experimental investigation of thermal performance in a tube with detached circular ring turbulators, Heat Transfer Eng, 33(8) (2012) 682-692.

[87] D. Bertsche, P. Knipper, T. Wetzel, Experimental investigation on heat transfer in laminar, transitional and turbulent circular pipe flow, Int. J. Heat Mass Transf., 95 (2016) 1008-1018.
[88] J.F. Barnes, J.D. Jackson, Heat transfer to air, carbon dioxide and helium flowing through smooth circular tubes under conditions of large surface/gas temperature ratio, Proceedings of the Institution of Mechanical Engineers: Part C, Journal of Mechanical Engineering Science, 3(4) (1961) 303-314.
[89] D.M. McEligot, Effect of large temperature gradients on turbulent flow of gases in the downstream region of tubes, PhD thesis, Stanford University, Stanford, 1963.
[90] F.M. White, Fluid Mechanics, 6th ed., McGraw-Hill, Singapore, 2009.
[91] G.K. Filonenko, Hydraulischer Widerstand von Rohrleitungen (Orig. Russ.), Teploenergetika, 1(4) (1954) 40-44.
[92] X. Fang, Y. Xu, Z. Zhou, New correlations of single-phase friction factor for turbulent pipe flow and evaluation of existing single-phase friction factor correlations, Nuclear Engineering and Design, 241 (2011) 897-902.
[93] W.L. Friend, A.B. Metzner, Turbulent heat transfer inside tubes and the analogy among heat, mass, and momentum transfer, AIChE Journal, 4(4) (1958) 393-402.
[94] D.T. Strickland, Heat transfer measurements in the transition region for a horizontal circular tube with a square-edged entrance, Master's dissertation, Oklahoma State University, Stillwater, 1990.
[95] S.W. Churchill, R. Usagi, A general expression for the correlation of rates of transfer and other phenomena, AIChE Journal, 18(6) (1972) 1121-1128.